

MONTHLY WEATHER REVIEW

JAMES E. CASKEY, JR., Editor

Volume 87
Number 11

NOVEMBER 1959

Closed January 15, 1960
Issued February 15, 1960

TEMPERATURE PATTERNS ALONG THE ATLANTIC AND GULF COASTS

ABRAM B. BERNSTEIN AND CHARLES R. HOSLER

Office of Meteorological Research, U.S. Weather Bureau, Washington D.C.

[Manuscript received September 21, 1959]

1. INTRODUCTION

As part of a recent survey of coastal climates of the United States, a study was made of air temperature patterns along the Atlantic coast and the Gulf of Mexico. This investigation serves as an example of the type of local climatological analysis that can be performed using existing data, without the need for setting up new and often costly observational programs. In addition, this study showed an interesting feature of the daily maximum temperature pattern—an "inland tongue" of high temperature—that does not appear on large scale maps of temperature distribution for the United States.¹

The data in this study were the average daily mean, maximum, and minimum temperature for approximately 500 cooperative observing stations, as well as first order Weather Bureau stations, along the Atlantic and Gulf coasts. Sources of data were *Climatic Summary of the United States—Supplement for 1931 through 1952* and *Local Climatological Data*, published by the U.S. Weather Bureau. Figures 1 and 2 show the networks of stations along the Atlantic and Gulf coasts, respectively.

Although the station network used in this study is quite dense, there were three major sources of difficulty. First, the various cooperative observing stations do not have a uniform period of record. An attempt was made to overcome this problem by eliminating stations with short

records (less than 5 years), and stations with inconsistencies caused by changes in station location. Second, stations are not equally distributed over different kinds of terrain—for example, there are few stations high up on mountain slopes—and there are differences in the temperature statistics due to differences of station exposure. To compensate for this, subjective smoothing was done in drawing isotherms. Also analyses of regions of sparse data were made in accordance with the temperature-altitude relationship which was evident in regions of dense data. Third, the absence of observations of air temperature over water made it difficult to analyze coastal areas and regions with inland bodies of water such as Long Island Sound, Chesapeake Bay, and Lake Ponchartrain.

Despite these data deficiencies, the networks were sufficiently dense to delineate features of the temperature patterns caused by local topographical features and bodies of water.

2. TEMPERATURE PATTERNS

The patterns of daily mean and minimum temperature appeared very much as expected. The mean temperature decreases with increasing elevation, and is higher over land in summer and higher over water in winter. These two effects, due to topography and land-water contrast, reinforce each other in winter and oppose each other in summer. The minimum temperature also decreases with elevation, and is higher over water than over land throughout the year.

The patterns of average daily maximum temperature show an unusual feature which merits examination in greater detail. The highest maximum temperature is

¹The latest edition of "Climates of the States", published by the U.S. Weather Bureau, includes maps showing the mean daily maximum and minimum temperatures for each State during January and July, based on data from the cooperative observing stations. The Atlantic and Gulf States for which these maps have been published as of December 1959 are Alabama, Florida, Georgia, Maine, and Massachusetts. The "Inland tongue" appears on these maps.

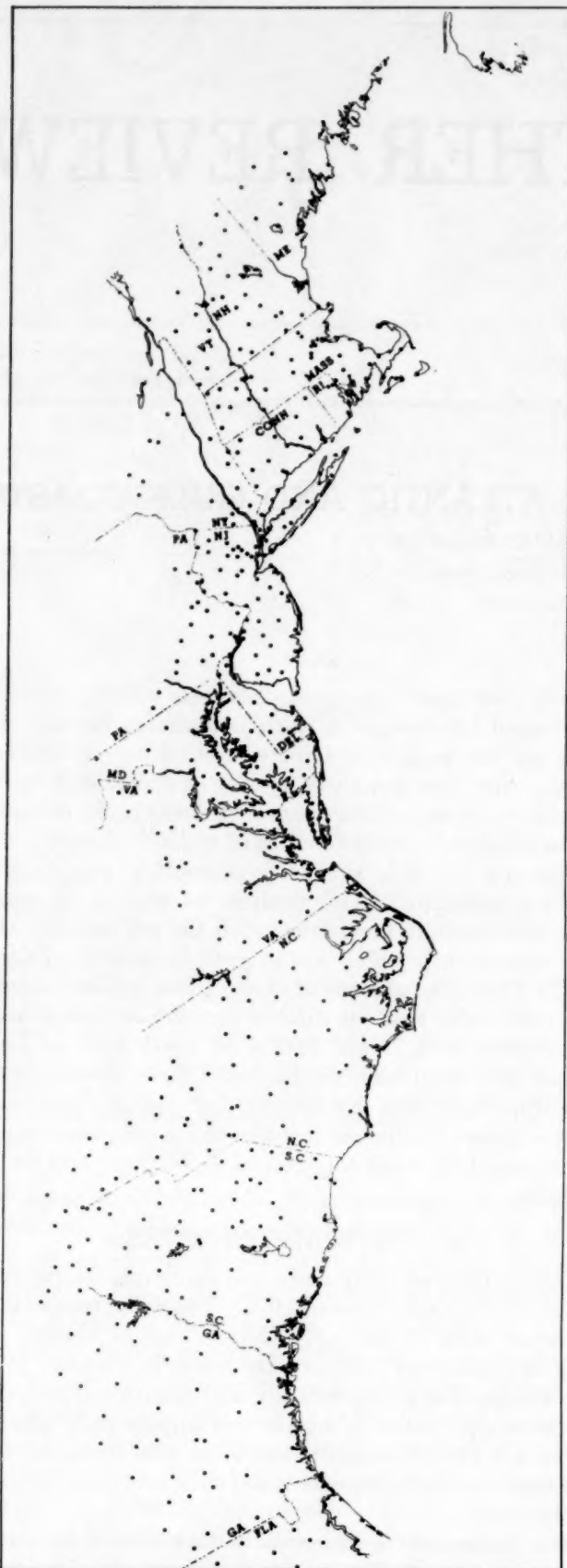


FIGURE 1.—Network of temperature stations along the Atlantic coast.

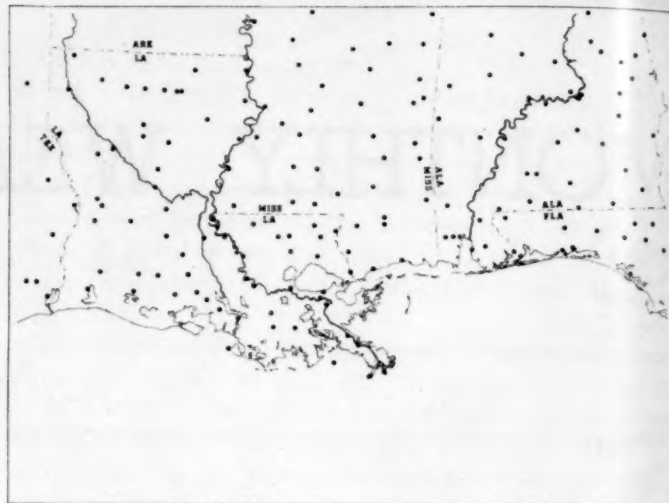


FIGURE 2.—Network of temperature stations along the Gulf coast.

found in a "belt" or "tongue" located about 25 to 75 miles inland from the coast. This "tongue" of relatively high temperature values, which is narrow and clearly defined in winter with pronounced horizontal temperature gradients, and quite broad in summer with weak horizontal temperature gradients, may be traced all along the Atlantic coast, as seen in figures 3-6. Only where the topography is complex, as in the New England area, does this "tongue" begin to lose its identity. Figure 7 indicates the main topographic features of the Atlantic seaboard.

It is reasonable to expect the daily maximum temperature to be higher over land than over water, and to decrease with increasing latitude and elevation. Figures 3-7 show that even the slight topographic slope (500 feet in about 250 miles) found in the middle and southern Atlantic States is sufficient to cause the daily maximum isotherms to be oriented from southwest to northeast, rather than from west to east. The fact that the highest temperature is found 25 to 75 miles inland, rather than along the coast, may be due to the transport of cooler ocean air inland by the afternoon sea breeze. If this is so, it is possible that the distance inland that the highest maximum temperature is found is an index of the average strength of the sea breeze in that area.

Along the Gulf coast the temperature analysis was less complicated, since the land is almost uniformly flat, the coastline is oriented west-to-east, and there are no strong water-temperature gradients offshore comparable to the Gulf Stream off the Atlantic coast. Consequently one would expect the isotherms to be oriented west-to-east with lower temperatures to the north, and any deviation from this must be due to topography or land-water contrast. The study showed that daily mean and minimum

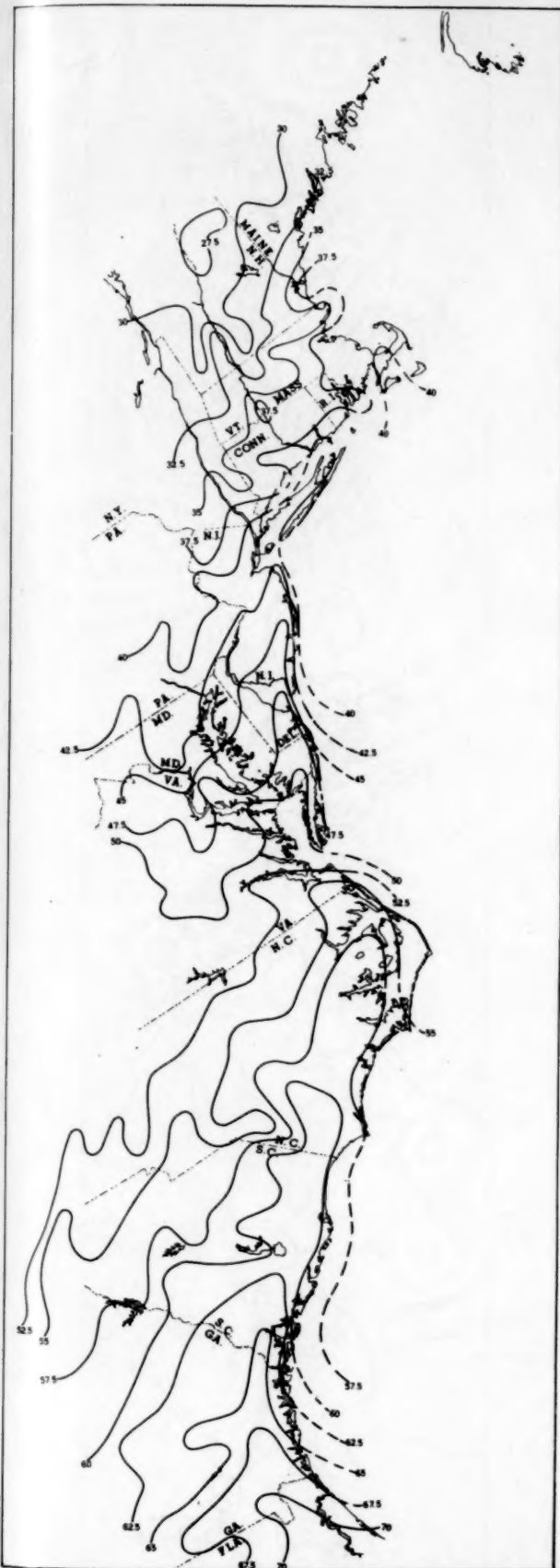


FIGURE 3.—Average daily maximum temperature ($^{\circ}\text{F}.$) along the Atlantic coast in January.

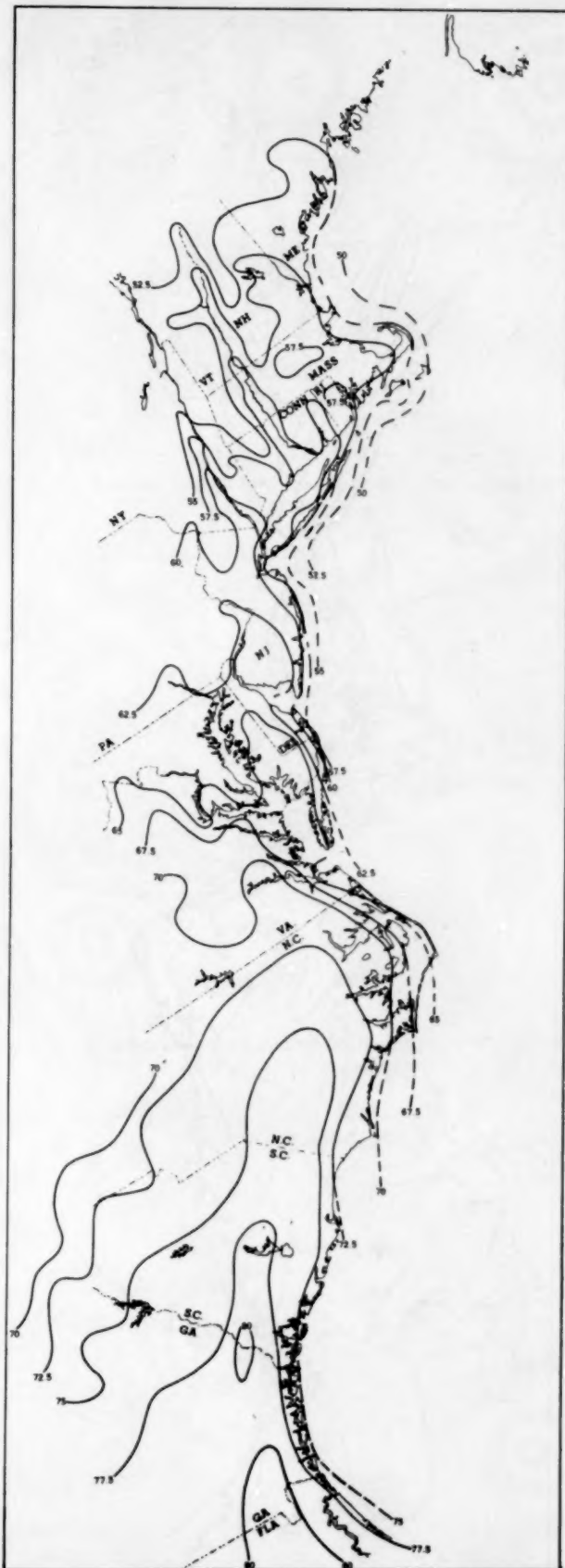


FIGURE 4.—Average daily maximum temperature ($^{\circ}\text{F}.$) along the Atlantic coast in April.



FIGURE 5.—Average daily maximum temperature ($^{\circ}$ F.) along the Atlantic coast in July.

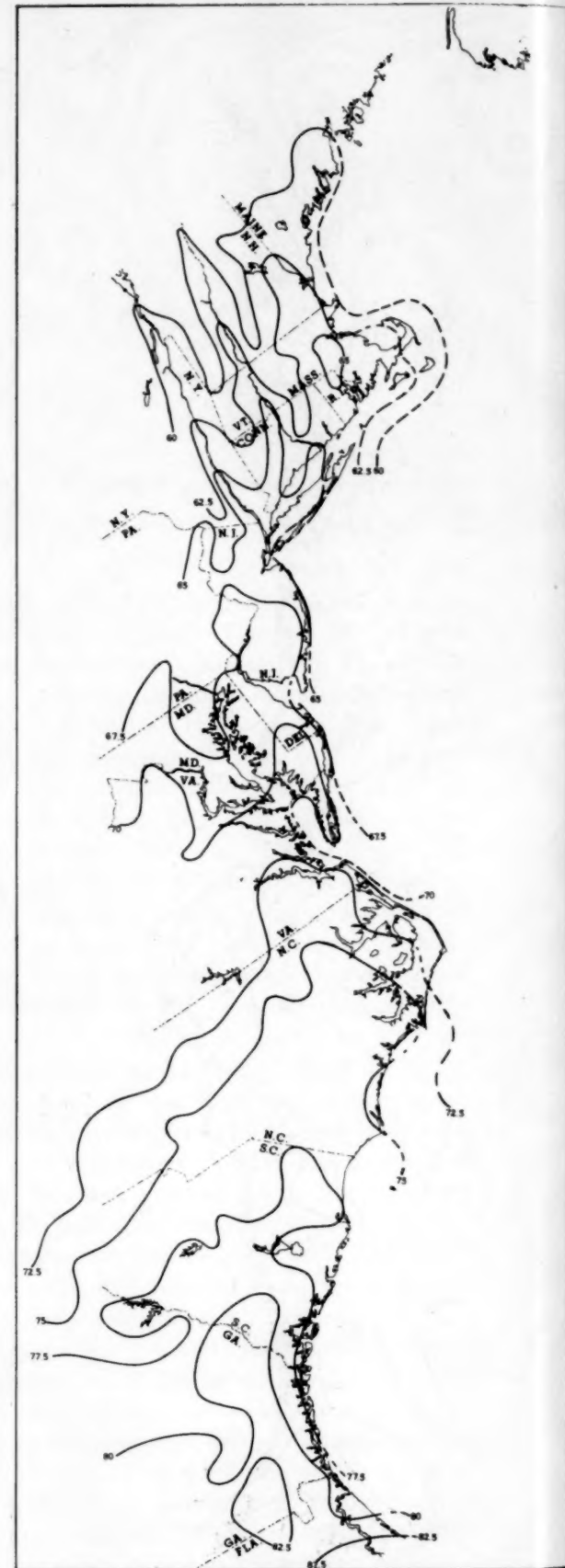


FIGURE 6.—Average daily maximum temperature ($^{\circ}$ F.) along the Atlantic coast in October.



FIGURE 7.—Topography of the Atlantic seaboard, showing 100-ft. and 500-ft. contours.

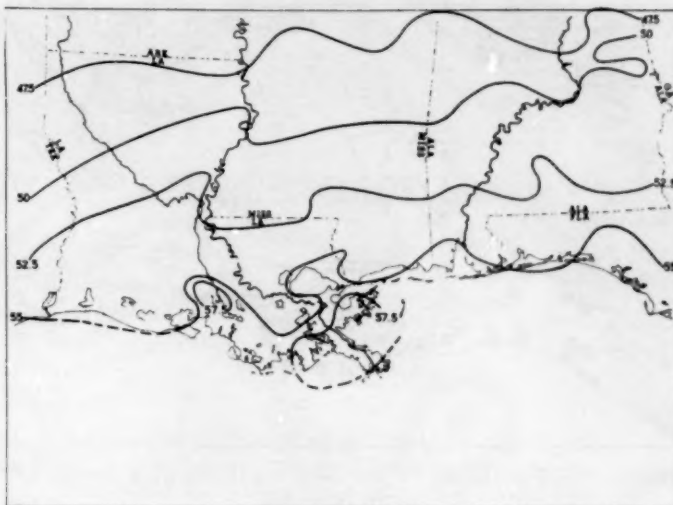


FIGURE 8.—Average daily mean temperature ($^{\circ}$ F.) along the Gulf coast in January.

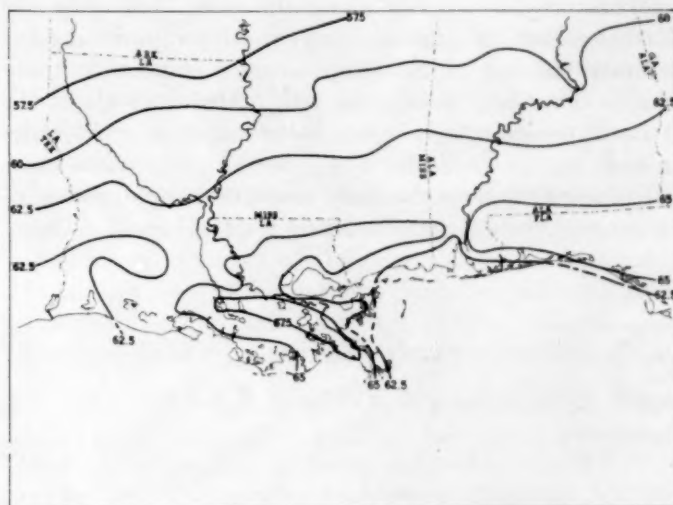


FIGURE 9.—Average daily maximum temperature ($^{\circ}$ F.) along the Gulf coast in January.

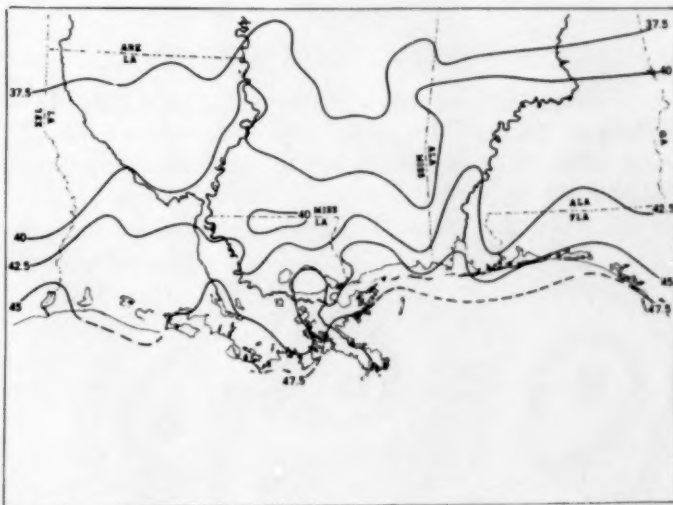


FIGURE 10.—Average daily minimum temperature ($^{\circ}$ F.) along the Gulf coast in January.

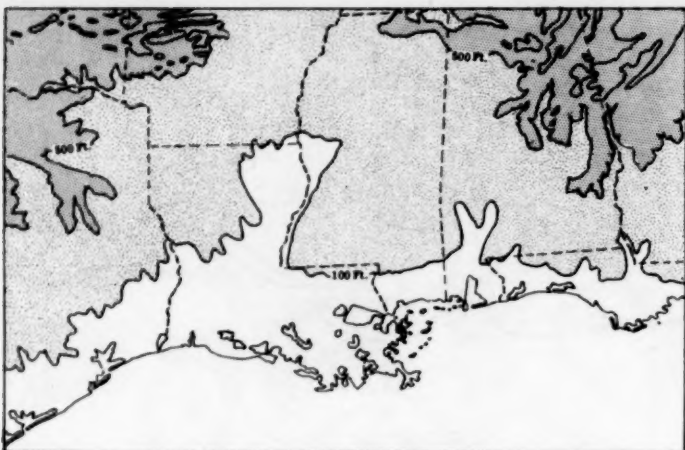


FIGURE 11.—Topography of the Gulf coast, showing 100-ft. and 500-ft. contours.

temperatures are higher along the coast than they are farther inland throughout the year, although during the summer the horizontal temperature variation is quite small. The daily maximum temperature, as along the Atlantic coast, is highest in a belt roughly 25 to 75 miles inland.

Figures 8–10 show the daily mean, maximum, and minimum temperature patterns along the Gulf coast in Janu-

ary. The land-water effect is quite evident in the vicinity of Lake Ponchartrain where the "inland tongue" of high maximum temperature is interrupted. The break in this "tongue" near Mobile is probably due to topography, as shown in figure 11.

3. CONCLUDING REMARKS

Despite several sources of difficulty with the data used in this study, the evidence of the "inland tongue" of high maximum temperatures is too strong to be ignored. Further, the data suggest that along the Atlantic coast the air temperature over bays and sounds rises as high during the afternoon as it does over land, while at night it does not fall as low. If this is so, it is probably due to mixing induced by stronger winds during the day, and the lack of mixing under stable conditions with light winds at night. However, this feature does not appear along the Gulf coast.

In the past there has been little climatological analysis of the local features of coastal regions, although the network of cooperative stations offers a long record of measurements of temperature and precipitation. It seems likely that a more extensive analysis of existing climatological data, especially in regions of lakes and mountains, may shed much light on the relation between local geography and climate.

in
high
this
as

ATMOSPHERIC TURBIDITY AT ATHENS, GREECE

GEORGE IAC. MACRIS

National Observatory, Athens, Greece¹

[Manuscript received May 18, 1959; revised October 28, 1959]

ABSTRACT

The turbidity of the cloudless sky at Athens, Greece, is investigated by means of pyrheliometric measurements made with No. 116 Kipp-Zonen pyrheliometer at the National Observatory, Athens. The measurements are based on observations of the direct sun radiation using two filters (red and yellow) and without a filter. The monochromatic turbidity is defined and used to compare the atmospheric transmission at Athens with the theoretical value for a Rayleigh (molecular) atmosphere. The results give an indication of the unique clarity of atmosphere in the Attica area.

1. INTRODUCTION

Local studies of the phenomena of solar radiation during its passage through the atmosphere are of great interest to all the physical sciences and particularly to meteorological physics. The study of the variation of intensity of solar radiation due to its attenuation by the atmosphere helps us to understand many physical characteristics of the structure and properties of the atmosphere. For example, from the turbidity we can draw some conclusions about the aerosol constitution of the atmosphere.

The purpose of this paper is to study daily variations of the turbidity of the atmosphere at Athens. The problem of the turbidity of the atmosphere is connected with the gradual extinction² of the solar radiation during its passage through the atmosphere [6], due to the absorption by gaseous constituents of the atmosphere, and the scattering by molecules and by larger particles that are known as aerosols, such as dust particles, sea salt particles, cloud droplets, etc. [11, 12]. This extinction or attenuation depends primarily on the length of the path of the solar radiation through the atmosphere. This depends on the zenith angle of the sun, as well as on the constitution of the atmosphere.

Regarding this problem some investigations have been carried out by Linke [8] and others. To determine the turbidity of the atmosphere, Linke evaluated the term $\frac{T'}{T}$, where T' is the observed or actual value of the optical thickness, and T the theoretical value of the Rayleigh or theoretical atmosphere (which is also often called the pure or molecular atmosphere). Although Linke based his study on the mean value of the optical thickness, he

did notice some very important characteristics of the transmission of the solar radiation in the atmosphere.

The present study, in which optical thickness values for each wavelength are used, is based on radiation data from the solar radiation station established at the National Observatory at Athens in 1953 at the suggestion of Professor E. Mariopoulos of the University of Athens [20]. Direct measurements of the solar energy are being made by using a No. 116 Kipp-Zonen pyrheliometer with yellow and red filters as well as with no filters. The transmitting regions of the filters used with the pyrheliometer are:

(1) yellow 28,000 Å, to 5,000 Å, (2) red 28,000 Å, to 6,000 Å. The pyrheliometer readings were taken at a specific time 11:20 (local civil time) only when the sky in the region of the sun was completely cloudless, which is usually expressed in S^4 in the Mörikofer Scale. (According to Mörikofer's Scale, S^0 means that the sun is completely obscured by clouds and S^4 means the sun is completely uncovered by clouds.)

2. DETERMINATION OF THE TURBIDITY

In this report, the values of the optical thickness were used for each wavelength, because it has been emphasized [15] that the effects of the transmission of solar energy will be more distinct if we use values of the turbidity factors for each wavelength by computation of the following ratios:

$$a = \frac{Q_B(\lambda) - Q_y(\lambda)}{Q'_B(\lambda) - Q'_y(\lambda)} = \frac{T_b}{T'_b}$$

$$b = \frac{Q_y(\lambda) - Q_r(\lambda)}{Q'_y(\lambda) - Q'_r(\lambda)} = \frac{T_y}{T'_y}$$

$$c = \frac{Q_y(\lambda)}{Q'_y(\lambda)}$$

$$p = \frac{Q_r(\lambda)}{Q'_r(\lambda)}$$

¹ Research performed during author's stay at University of California, Los Angeles, Calif.

² The annual depletion of the solar energy at Athens, Greece, was studied in reference [10].

where

$Q'_B(\lambda)$ and $Q_B(\lambda)$ denote the actual and theoretical amount, respectively, of solar energy in the spectral region $0.3 \leq \lambda \leq 2.8\mu$ (white light), falling on a normal surface at sea level in ly./min. (gram-calories per cm.² per min.)

$Q'_y(\lambda)$ and $Q_y(\lambda)$ denote the actual and theoretical amount, respectively, of solar energy in the spectral region $.515 \leq \lambda \leq 2.8\mu$ (yellow filter of the instrument) falling on a normal surface at sea level in ly./min.

$Q'_r(\lambda)$ and $Q_r(\lambda)$ denote the actual and theoretical amount, respectively, of solar energy in the spectral region $.625 \leq \lambda \leq 2.8\mu$ (red filter of the instrument) falling on a normal surface at sea level in ly./min.

The ratio $\frac{T_b}{T'_b}$ will be defined as the turbidity for the spectral region $.3 \leq \lambda \leq .515\mu$. The ratio $\frac{T_y}{T'_y}$ is for the spectral region $.515 \leq \lambda \leq .625\mu$. Also the ratio $\frac{Q_y}{Q'_y}$ is called the turbidity for the spectral region of the yellow filter of the instrument $.515 \leq \lambda \leq 2.8\mu$ and the ratio $\frac{Q_r}{Q'_r}$, is called the turbidity for the particular spectral region of the red filter of the instrument $.625 \leq \lambda \leq 2.8\mu$. Since the values of $Q'(\lambda)$ were determined from the pyrheliometric measurements, in our problem the theoretical values of $Q(\lambda)$ only are to be computed.

These values can be obtained by evaluating the integral

$$Q(\lambda_1, \lambda_2) = \int_{\lambda_1}^{\lambda_2} I_o(\lambda) T(\lambda) d\lambda \quad (1)$$

where λ_1 and λ_2 represent the wavelength limits which apply, $I_o(\lambda)$ is the specific intensity of solar radiation, and $T(\lambda)$ is the fractional transmission of the filter, both at the wavelength λ . Expression (1) then represents the extraterrestrial theoretical values of the amount of the solar energy at the top of the atmosphere received through the filter of transmission $T(\lambda)$.

To apply the above computation to the surface of the earth it has to be formulated in the following way:

$$Q(\lambda_1, \lambda_2) = \int_{\lambda_1}^{\lambda_2} I_o(\lambda) T(\lambda) e^{-\tau \sec \theta} d\lambda \quad (2)$$

where $e^{-\tau \sec \theta}$ is the transmission coefficient as given from the extension of the Bourger-Langley law for the pure molecular atmosphere [2, 16, 17, 18, 19]. These coefficients were obtained by interpolating values of monochromatic normal thickness for pure molecular atmosphere as given by Deirmendjian [3, 4]. The expression for the optical thickness τ is

$$\tau = \int_0^\infty b_\lambda dz \quad (3)$$

TABLE 1.—Optical thickness (τ) of the molecular atmosphere as function of the wavelength (λ in microns)

λ	τ	λ	τ	λ	τ
0.305	1.0295	0.605	0.0667	0.905	0.0131
0.355	0.7484	0.655	0.0468	0.955	0.0109
0.405	0.4465	0.705	0.0346	1.025	8.79×10^{-4}
0.455	0.2122	0.755	0.0264	1.525	1.55×10^{-4}
0.505	0.1388	0.805	0.0204	2.025	4.96×10^{-4}
0.555	0.0972	0.855	0.0162	2.425	2.41×10^{-4}

where b_λ is the monochromatic attenuation coefficient, a function of the density and the refractive index of the atmospheric layer. z is the normal distance measured vertically above the sea level; see θ is the factor often called air mass, where θ is the zenith distance of the sun.

The values of $I_o(\lambda)$ were determined graphically from Nicolet's table [13, 14]. The transmission $T(\lambda)$ of the filters was determined from tables for standard European red and yellow filters [1]. For greater accuracy both graphs were expanded. The values were plotted on separate graphs as a function of λ for the yellow and red filters. By interpolation the transmission of the filters for different wavelengths was obtained with an accuracy of 0.001. In the integration (2) the trapezoidal rule was used with $\Delta\lambda=100\text{ \AA}$.

The values of the optical thickness were used from the theoretical computations by Deirmendjian and Sekera [4, 5]. These values were plotted versus wavelength on logarithmic paper. In table 1 these values of the optical thickness are given as a function of wavelength. From the plot, the optical thicknesses for all the wavelengths in the regions of the filters were determined accurately to 0.001. Then the transmission coefficient was computed for the values of zenith distance varying from maximum solar altitude at the latitude of the solar radiation station at Athens, Greece. That is, the extinction coefficient was computed for the following values of the zenith distance $\theta=15^\circ, 30^\circ, 45^\circ, 50^\circ, 55^\circ, 60^\circ, 65^\circ$, and 70° .

3. DISCUSSION OF THE NUMERICAL RESULTS

Using these extinction coefficients we are able to perform the integration (2) by numerical methods, using the trapezoid rule with $\Delta\lambda=100\text{ \AA}$. The final answers are recorded in table 2. These values express the amount of solar energy (ly./min.) that is received by a surface, normal to the rays, of one square centimeter at sea level for a pure molec-

TABLE 2.—The variation of the transmission of the solar energy (ly./min.) in a Rayleigh atmosphere as a function of wavelength and zenith distance

Spectral region	λ (in microns)	Zenith distance							
		15°	30°	45°	50°	55°	60°	65°	70°
White.....	0.300-2.800	1.802	1.785	1.751	1.734	1.714	1.686	1.651	1.599
Yellow filter.....	0.515-2.800	1.283	1.278	1.268	1.263	1.256	1.247	1.234	1.215
Red filter.....	0.625-2.800	1.049	1.047	1.043	1.040	1.037	1.033	1.027	1.018

ular atmosphere and for the indicated zenith distances. From these numerical values the three curves I, II, III in figure 1 were plotted. Curve I represents the region of wavelengths from 0.300 to 2.800 μ . Curve II represents the region of wavelengths from 0.515 to 2.800 μ (yellow filter of the instrument). Curve III represents the region of wavelengths from 0.625 to 2.800 μ (red filter of the instrument). Thus, from the curves we are able to determine the values of the solar energy in ly./min. received by a normal surface of one square centimeter at sea level, and for any values of the zenith distance contained between the extreme values 15° to 70°, and of course for all the corresponding altitudes of the sun that are included in these two values.

Finally, we computed the ratios a , b , c , d , using for Q' values obtained during the period 1953 to 1957 from daily observations at 11:20 local civil time and for Q the corresponding theoretical values (same λ and elevation). The plot of these values versus the months is given in figure 2 for the spectral region 0.300 to 0.515, in figure 3 for the spectral region 0.515 to 0.625, in figure 4 for the yellow filter, and in figure 5 for the red filter. Figures 2-5 represent the computed turbidity for observations during a particular month separately for each of the years 1953-1957, with the total number of observations in a particular month given in the bottom line. The results we obtained can be summarized as follows:

1.—In figures 2-5 (except figure 3 in which it is not so clear) a simple annual variation in the turbidity of the atmosphere in Athens is clearly visible. This variation shows a maximum in the summer season and a minimum in the winter or early spring (March). The increased turbidity in summer months is most likely caused by an increase in the number of aerosol particles, as well as by an increase in the size of the particles due to the greater relative humidity in the summer. This is caused by the south to southwest wind and the high frequency of sea breezes bringing more water vapor over Athens. These interpretations apply to average conditions. It can be seen in figure 2 that there are exceptions to this and very low turbidity can occur on some summer days as well as high turbidity during some winter days. This results in increased absorption and scattering of solar energy.

The accumulation of aerosols during the summer months is due to many factors. Some of the more important ones are (1) the number of days of precipitation is very small [9, 20] and therefore only a small scavenging effect can be expected; (2) the sea breeze brings (a) aerosols from the industrial district over to Athens and (b) dust particles raised up by whirl winds which are caused by an interaction of northeast and southwest breeze; (3) the increased turbulence during the summer months raises dust from the dried inland vegetation.

2.—From figures 2 and 3 we can say that the deviation of the radiation characteristics of a turbid atmosphere from

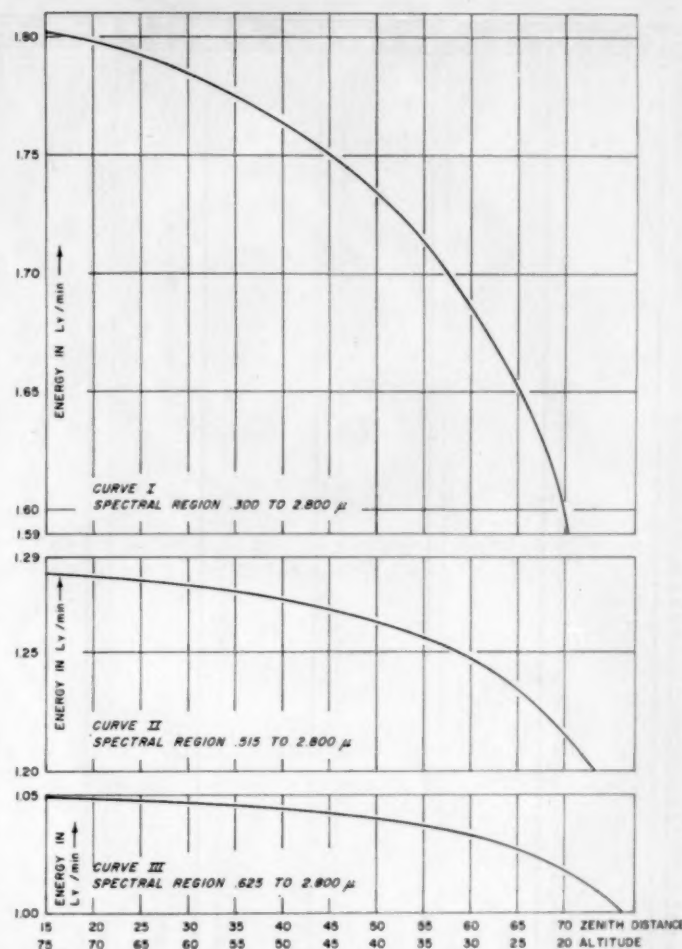


FIGURE 1.—Curves showing the variation of solar energy in a Rayleigh atmosphere with respect to zenith distance. Curve I is for white light; Curve II, using a yellow filter; and Curve III using a red filter.

that of a pure molecular atmosphere increases with the wavelength.

3.—The consequence of the above results is that the values of turbidity in the spectral region 0.300 to 0.515 μ , figure 1, are smaller than the values of the turbidity as given in figures 3, 4, and 5. This indicates that the atmosphere in Athens under clear conditions does not differ from the pure molecular atmosphere. The reason for that probably is this: The atmosphere over the Attica area is very dry (the driest of all Greece) as indicated from the observations of the relative humidity [9]. This probably explains the famous "Cyan" of the deep blue of the sky of Athens under clear conditions. Some earlier investigations of the blueness of the sky at Athens, Greece, were reported by L. Karapiperis and Ph. Karapiperis [7].

4.—Moreover, figures 2-5 confirm the results of turbidity determination from the measurements of sky light polarization performed under the direction of Prof. Z. Sekera at the University of California, Los Angeles [21].

	January 53 54 55 56 57	February 53 54 55 56 57	March 53 54 55 56 57	April 53 54 55 56 57	May 53 54 55 56 57	June 53 54 55 56 57	July 53 54 55 56 57	August 53 54 55 56 57	September 53 54 55 56 57	October 53 54 55 56 57	November 53 54 55 56 57	December 53 54 55 56 57
2.00										1		
1.99												
1.98												
1.97												
1.96												
1.95												
1.94												
1.93												
1.92												
1.91												
1.90												
1.89												
1.88												
1.87												
1.86												
1.85												
1.84												
1.83												
1.82												
1.81												
1.80												
1.79												
1.78												
1.77												
1.76												
1.75												
1.74												
1.73												
1.72												
1.71												
1.70												
1.69												
1.68												
1.67												
1.66												
1.65												
1.64												
1.63												
1.62												
1.61												
1.60												
1.59												
1.58												
1.57												
1.56												
1.55												
1.54												
1.53												
1.52												
1.51												
1.50												
1.49												
1.48												
1.47												
1.46												
1.45												
1.44												
1.43												
1.42												
1.41												
1.40												
1.39												
1.38												
1.37												
1.36												
1.35												
1.34												
1.33												
1.32												
1.31												
1.30												
1.29												
1.28												
1.27												
1.26												
1.25												
1.24												
1.23												
1.22												
1.21												
1.20												
1.19												
1.18												
1.17												
1.16												
1.15												
1.14												
1.13												
1.12												
1.11												
1.10												
1.09												
1.08												
1.07												
1.06												
1.05												
1.04												
1.03												
1.02												
1.01												
1.00												
Total	3 6 6 5 5	8 5 8 5 8	8 2 9 5 -	13 5 8 14 10	8 9 15 14 9	17 22 22 20 21	24 27 25 26 26	29 27 19 29 24	25 28 14 20 13	10 11 7 20 8	6 7 9 5 5	5 6 8 13 4

FIGURE 2.—Annual variation of the turbidity in the spectral region, 0.300 to 0.515 μ at Athens, Greece. The observation plotted at 2.00 is equal to 2.09.

	January 55 54 55 56 57	February 55 54 55 56 57	March 55 54 55 56 57	April 55 54 55 56 57	May 55 54 55 56 57	June 55 54 55 56 57	July 55 54 55 56 57	August 55 54 55 56 57	September 55 54 55 56 57	October 55 54 55 56 57	November 55 54 55 56 57	December 55 54 55 56 57
2.12	1 1	1	1	1 2 .	2	2 1 2	1 1	3 1 1 1	1 3 1 1	1 3	1 2 1	2 1
2.11					1 4 2	5 4 2	1 3 2	1 2 3 1	1			1
2.10	1					1						
2.09												
2.08												
2.07												
2.06												
2.05												
2.04												
2.03												
2.02												
2.01												
2.00												
1.99												
1.98												
1.97												
1.96												
1.95												
1.94												
1.93												
1.92												
1.91	2 1	1	2	1 2	1 2 1	2 2 3 1 2	2 2 3 7 4	1 2 4 4	1 4 1 2	1 2		1 2
1.90												
1.89												
1.88												
1.87												
1.86												
1.85												
1.84												
1.83	1 1 2	2										
1.82												
1.81												
1.80												
1.79												
1.78												
1.77												
1.76	2 1 1 1	1 1 1	3 1 2	1 4 4 2	3 4 7 4 3	2 7 4 11 2	5 6 6 2 7	5 1 3 2	1 4		1	1 1 1 1
1.75												
1.74												
1.73												
1.72												
1.71												
1.70												
1.69	1 1	2 2	1									
1.68												
1.67												
1.66												
1.65												
1.64												
1.63												
1.62	2 1 1 1	1										1 6
1.61												
1.60												
1.59												
1.58												
1.57	1 2 4 2	5 2 2 1 2	1 1	1 2								3 4
1.56												
1.55												
1.54												
1.53												
1.52												
1.51												
1.50												
1.49												
1.48												
1.47	1 1 1 3	1 1 1 5 1	1 1 2 1	4 2 3 3 4	8 7 2 4	4 6 9 2 3						
1.46												
1.45												
1.44												
1.43												
1.42												
1.41												
1.40												
1.39												
1.38	1	1	1 1	1								
1.37												
1.36												
1.35												
1.34												
1.33												
1.32												
1.31	1	2										
1.30												
1.29												
1.28	1	2	1 1	1								
1.27												
1.26												
1.25												
1.24												
1.23												
1.22												
1.21												
1.20												
1.19												
1.18												
1.17												
1.16												
1.15												
1.14												
1.13												
1.12												
1.11												
1.10												
1.09												
1.08												
1.07												
1.06												
1.05												
1.04												
1.03												
1.02												
1.01												
1.00	1				1							
Total	4 7 6 6 7	9 5 8 5 9	9 2 9 5	13 7 8 10	8 9 15 24 9	17 22 22 20 19	26 28 23 26 26	23 27 19 30 24	26 28 14 25 13	30 31 6 21 3	7 7 9 6 6	6 6 6 15 6

FIGURE 3.—Annual variation of the turbidity in the spectral region 0.515 to 0.625 μ at Athens, Greece. The observations plotted at 2.12 have a range from 2.20 to 5.75.

FIGURE 4.—Annual variation of the turbidity in the spectral region 0.515 to 2.800 μ at Athens, Greece. The observations plotted at 2.00 are equal to 2.13.

	January 55 54 55 56 57	February 55 54 55 56 57	March 55 54 55 56 57	April 55 54 55 56 57	May 55 54 55 56 57	June 55 54 55 56 57	July 55 54 55 56 57	August 55 54 55 56 57	September 55 54 55 56 57	October 55 54 55 56 57	November 55 54 55 56 57	December 55 54 55 56 57
5.00								1				1
1.99								1				
1.98												
1.97												
1.96												
1.95												
1.94												
1.93												
1.92												
1.91												
1.90												
1.89												
1.88												
1.87												
1.86												
1.85												
1.84												
1.83												
1.82												
1.81												
1.80												
1.79												
1.78												
1.77												
1.76												
1.75												
1.74												
1.73												
1.72												
1.71												
1.70												
1.69												
1.68												
1.67												
1.66												
1.65												
1.64												
1.63												
1.62												
1.61												
1.60												
1.59												
1.58												
1.57												
1.56												
1.55												
1.54												
1.53												
1.52												
1.51												
1.50												
1.49												
1.48												
1.47												
1.46												
1.45												
1.44												
1.43												
1.42												
1.41												
1.40												
1.39												
1.38												
1.37												
1.36												
1.35												
1.34												
1.33												
1.32												
1.31												
1.30												
1.29												
1.28												
1.27												
1.26												
1.25												
1.24												
1.23												
1.22												
1.21												
1.20												
1.19												
1.18												
1.17												
1.16												
1.15												
1.14												
1.13												
1.12												
1.11												
1.10												
1.09												
1.08												
1.07												
1.06												
1.05												
1.04												
1.03												
1.02												
1.01												
1.00												
Total	4 7 6 6 7	9 5 8 5 9	9 2 9 5	13 7 8 14 10	8 0 15 14 9	17 22 22 20 21	27 26 23 26 26	26 27 19 20 28	26 28 18 25 15	10 11 7 20 3	6 7 9 6 6	6 6 8 15 6

FIGURE 5.—Annual variation of the turbidity in the spectral region 0.625 to 2.800 μ at Athens, Greece. The observations plotted at 2.00 are equal to 2.02.

5.—Special interesting features are displayed by figure 3 as compared to figure 2. In figure 3 (spectral region 0.515 to 0.625 μ) it is clearly shown that a certain distinctive degree of turbidity prevails during the winter and summer seasons. These turbidity values remained the same in the period 1953 to 1957. The values which appear to be more pronounced during the period March to October are about 1.44, 1.53, 1.64, 1.77, 1.92, 2.09; during the period September to December and January to February they are about 1.46–1.47, 1.57, 1.62, 1.69, 1.75. It seems as if this structure in the turbidity values is caused by special properties in the size distribution of the aerosols which appears to be constant for a particular air mass invading the Attica area.

This study proves quite clearly the advantages of the study of monochromatic turbidity [15, 16] and its potentialities in the study of relationships between the turbidity and the weather.

ACKNOWLEDGMENTS

The author wishes to acknowledge his gratitude to Professor Z. Sekera of the University of California at Los Angeles for suggesting this study and for his continuous interest and help during the work on this problem.

This work would not have been possible without the kind invitation of Professor J. Bjerknes and the kindness of Professor M. Neiburger, Chairman of the Department, in providing the author with all the necessary conveniences.

REFERENCES

1. F. Baur et al., *Linkes Meteorologisches Taschenbuch*, vol. 2, New edition, Geestand Portig, Leipzig 1953, 724 pp. (See p. 520.)
2. F. Bernhardt, "Die Sekundär-diffuse Strahlung in einer Rayleigh-Atmosphäre," *Zeitschrift für Meteorologie*. I: vol. 6, 1952, pp. 257–271. II: vol. 7, 1953, pp. 78–85.
3. D. Deirmendjian, "Attenuation of Light in the Earth's Atmosphere and Related Problems," *Scientific Report No. 1*, on Contract AF 19(122)-239, University of California, Dept. of Meteorology, 1952, 32 pp.
4. D. Deirmendjian, "The Optical Thickness of the Molecular Atmosphere," *Archiv für Meteorologie, Geophysik und Bioklimatologie*, Serie B, Band 6, Heft 4, 1955, pp. 452–461.
5. D. Deirmendjian and Z. Sekera, "Global Radiation Resulting from Multiple Scattering in a Rayleigh Atmosphere," *Tellus*, vol. 6, No. 4, Nov. 1954, pp. 382–398.
6. S. Fritz, "Solar Radiant Energy and Its Modification by the Earth and Its Atmosphere," *Compendium of Meteorology*, American Meteorological Society, Boston, Mass., 1951, pp. 13–33.
7. L. Karapiperis and Ph. Karapiperis, "Peri tou Kyanou Chōmatos tou ouranour en Athénais [On the Blueness of the Sky at Athens], *Praktika, Akademia Athēnōn*, vol. 27, 1952, pp. 211–215.
8. F. Linke, "Die Sonnenstrahlung und ihre Schwächung in der Atmosphäre," *Handbuch der Geophysik*, Band 8, Gebr. Borntraeger, Berlin, 1942, 1943.
9. E. G. Mariopoulos, *The Climate of Greece*, A. A. Papaspyros, Athens, Greece, 1938.
10. G. Macris, "Solar Energy and Sunshine Hours at Athens, Greece," *Monthly Weather Review*, vol. 87, No. 1, Jan. 1959, pp. 29–32.
11. M. Neiburger, "The Reflectivity of the Sea Surface for Diffuse Radiation," *Transactions, American Geophysical Union*, vol. 29, 1948, pp. 647–652.
12. M. Neiburger, "Reflection, Absorption, and Transmission of Insolation by Stratus Cloud," *Journal of Meteorology*, vol. 6, No. 2, Apr. 1949, pp. 98–104.
13. M. Nicolet, "La mesure du rayonnement solaire," Institut Royal Meteorologique du Belgique, *Miscellanées*, Fasc. xxi, 1948, pp. 3–37.
14. M. Nicolet, "Sur la détermination du flux énergétique du rayonnement extraterrestre du Soleil," *Archiv für Meteorologie, Geophysik und Bioklimatologie*, Serie B, vol. III, Number 3, 1951, pp. 209–219.
15. Z. Sekera, "Polarization of Skylight," *Handbuch der Physik*, vol. 48, 1957, pp. 288–327.
16. Z. Sekera, "Polarization of Skylight," *Compendium of Meteorology*, American Meteorological Society, Boston, Mass., 1951, pp. 79–90.
17. J. W. Strutt (Lord Rayleigh), "On the Light from the Sky, its Polarization and Colour," *Philosophical Magazine*, vol. 41, 4th series, 1871, pp. 107–120, 274–279.
18. Lord Rayleigh, "On the Electromagnetic Theory of Light," *Philosophical Magazine*, vol. 42, 5th series, 1881, pp. 81–101.
19. Lord Rayleigh, "On the Transmission of Light through an Atmosphere Containing Small Particles in Suspension, and on the Origin of the Blue of the Sky," *Philosophical Magazine*, vol. 47, 5th Series, 1899, pp. 375–384.
20. National Observatory, *Climatological Bulletin*, Athens, Greece.
21. University of California at Los Angeles, Dept. of Meteorology, "Investigation of Polarization of Skylight," *Final Report on Contract AF 19(122)-239*, June 1955, 68 pp.

FRONTAL PASSAGES OVER THE NORTH ATLANTIC OCEAN

GEORGIA C. WHITING

National Weather Records Center, U.S. Weather Bureau, Asheville, N.C.

[Manuscript received September 8, 1959; revised October 27, 1959]

ABSTRACT

Graphical and tabular data on the frequency of frontal passages at Ocean Station Vessels on the North Atlantic are compiled from historical weather maps for the years 1945-57. The stabilizing influence of the Gulf Stream is shown by the rapid modification of air temperature at all stations and by the rapid transition of frontal systems. The greatest frequency of fronts is found at the line of initial contact of cooler air with that associated with the Gulf Stream in the westernmost region of the ocean.

The value of the historical sea level synoptic weather maps as a data source for the climatological study of atmospheric motion systems is emphasized.

1. INTRODUCTION

The air mass theory of modern meteorology was offered by Bjerknes [1] in 1919. Bjerknes's concept, though modified over the years, continues as a basic approach to the analysis of daily surface or "sea level" synoptic weather maps [7]. The boundaries or leading edges of air masses, generally known as "fronts," are regularly entered on surface weather maps. Because fronts often produce notable weather changes as they pass by an individual location, the past, present, and anticipated positions of fronts bear heavily on the daily weather forecast.

Fronts, air masses, and other dynamic features of the general circulation, presently indispensable to daily weather map analysis and forecasting, are also useful in explaining climate in qualitative terms. These features are not, however, so amenable to statistical analysis of climate. Air masses particularly are subject to labeling that differs among analysts. Likewise the placement of fronts on a weather map is subject to individual interpretation. As a result, there have been but few efforts to analyze these features systematically as climatic elements. However, the careful preparation of an historical series of daily weather maps offers a far greater potential for consistency and continuity than those prepared on an operational basis.

The program for preparing the first series of such maps during World War II [11] and some of their derivatives (many still unpublished) was reported by Wexler and Tepper [16]. During the war, as the first 10 years of the series became available (1929-38), a great many statistics on fronts, cyclones, anticyclones, deepening and filling and tracks of Lows, etc. [2, 3, 13, 14, 15] were compiled. A

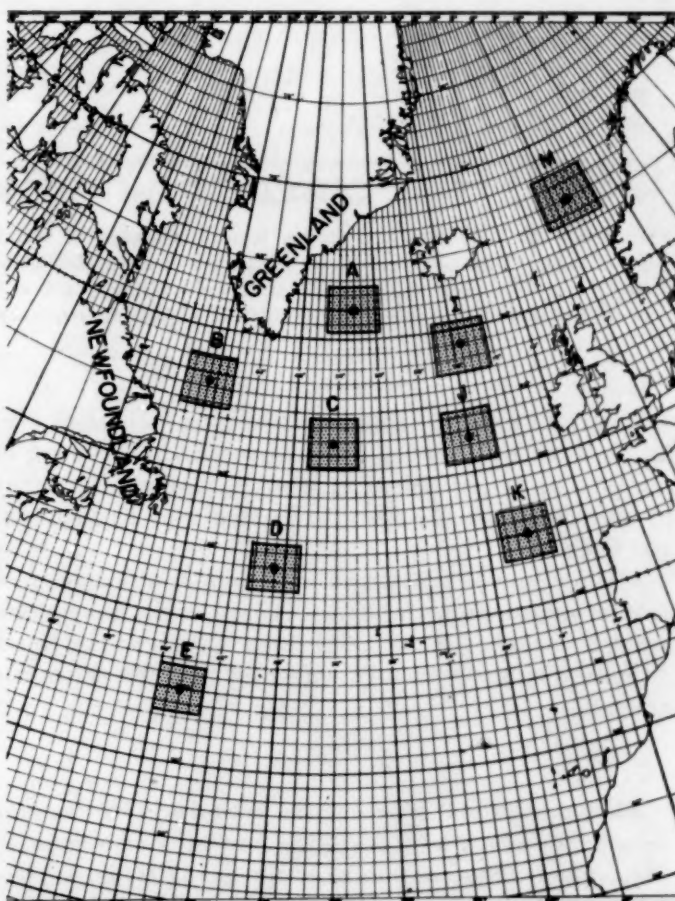


FIGURE 1.—Presently assigned Ocean Station Vessel positions in the North Atlantic, with position center point circumscribed by "on-station" limits. These are the areas used in tabulating frontal passages.

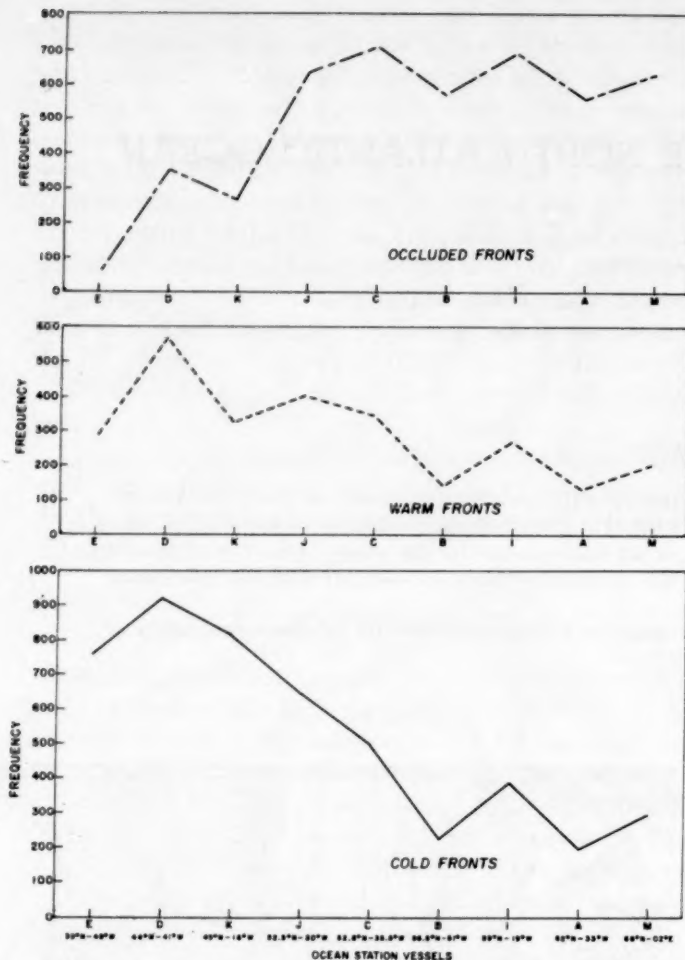


FIGURE 2.—Total frequency of major frontal passages at North Atlantic Ocean Station Vessels for the period October 1945–June 1957. Stations are arranged to show the latitudinal progression of fronts as well as areas of maximum and minimum frequency.

summary of some of these data was later published [12] by the U.S. Navy under whose sponsorship the work of compilation had been done. Other examples of the utility of such maps are the work of Gregor and Krivsky [4] and Klein [5].

The purpose of this paper is to present a summary of frontal systems from the sea level charts of the more recent years in the map series [9, 10] for a portion of the North Atlantic Ocean frequently traversed by both ships and aircraft.

2. DATA

Eleven years and nine months (October 1945 through June 1957) of sea level maps are used as source material [6]. These maps are published for the 1230 GMT surface synoptic observations; i.e., at 24-hour intervals. Generally only major fronts are drawn on the maps. For the most part minor fronts do not appear unless uniquely significant. Beyond the scope of analysis in the historical

TABLE 1.—*Monthly frequency of frontal passages at Ocean Station Vessels by frontal type, for the period October 1945–June 1957*

Station	Jan.	Feb.	Mar.	Apr.	May	June	July	Aug.	Sept.	Oct.	Nov.	Dec.
Cold Fronts												
A	28	16	23	16	14	8	12	11	18	16	22	13
B	17	18	17	15	18	16	27	19	28	25	14	16
C	48	36	32	43	33	33	56	35	45	48	46	48
D	80	72	71	84	79	82	66	76	86	68	62	60
E	94	88	111	72	64	32	14	18	41	68	64	68
I	46	28	43	38	33	21	21	16	26	40	40	33
J	69	47	47	60	46	48	47	50	48	57	55	74
K	81	64	48	68	69	62	49	75	78	69	70	80
M	27	19	48	34	22	17	14	17	23	30	21	26
Warm Fronts												
A	16	14	14	12	4	5	10	6	15	9	17	10
B	9	12	7	6	7	10	30	9	19	11	10	13
C	40	20	19	31	14	28	50	28	24	23	34	33
D	49	35	45	60	51	54	45	57	50	35	33	35
E	31	42	40	31	18	15	4	4	9	26	30	32
I	32	19	27	22	22	10	19	10	18	27	26	34
J	47	29	32	37	26	36	36	33	27	23	32	43
K	44	33	24	20	23	23	12	42	29	21	26	24
M	21	11	32	21	13	10	5	7	16	24	19	29
Occluded Fronts												
A	50	39	51	47	55	38	31	45	32	60	45	64
B	45	35	33	45	42	48	43	53	55	69	61	44
C	68	57	59	61	65	59	38	55	49	70	58	75
D	47	42	51	31	40	16	5	5	15	29	33	38
E	10	10	5	8	3	1	0	0	0	1	4	9
I	78	47	51	61	43	62	55	50	47	72	48	78
J	71	51	45	52	48	53	45	46	52	54	54	66
K	34	21	36	18	23	23	14	11	18	20	25	27
M	64	47	48	76	37	34	45	33	49	68	56	74
Stationary Fronts												
A	0	6	3	4	0	3	1	1	5	2	2	1
B	0	0	4	1	2	2	4	7	3	3	2	0
C	4	7	3	3	0	0	2	1	3	6	2	2
D	6	6	7	11	2	8	9	11	8	10	3	9
E	5	3	7	7	10	7	1	3	10	12	9	11
I	2	5	4	2	3	4	1	1	2	3	1	0
J	2	2	2	2	4	3	4	2	2	5	5	1
K	7	4	4	4	2	5	3	1	3	6	4	6
M	3	2	4	3	2	5	0	4	4	3	1	1

series are occasional redevelopments or frontolyses which take place within the 24 hours. Nevertheless the consistency that is maintained in this historical series of maps permits relatively systematic climatological treatment. Reference points for compiling the frontal frequencies discussed here are those locations presently assigned in the North Atlantic Ocean Station Network (see fig. 1), although vessels have not been located at these exact positions all through the period used. By the use of plastic masks, upon which the Ocean Station Vessel positions and "on-station squares" were printed in the correct scale, the fronts could be followed from day to day through the station squares. Checks were employed to guard against tabulating errors.

The following frontal types were considered: cold, warm, occluded, and stationary. An attempt to discriminate between cold and warm occlusions was abandoned because of the relative paucity of ship's observations. Data for stationary fronts are not presented separately, but are included in the graphs for all fronts combined.

Type of front and date of frontal passage at each Ocean Station Vessel position were recorded along with the

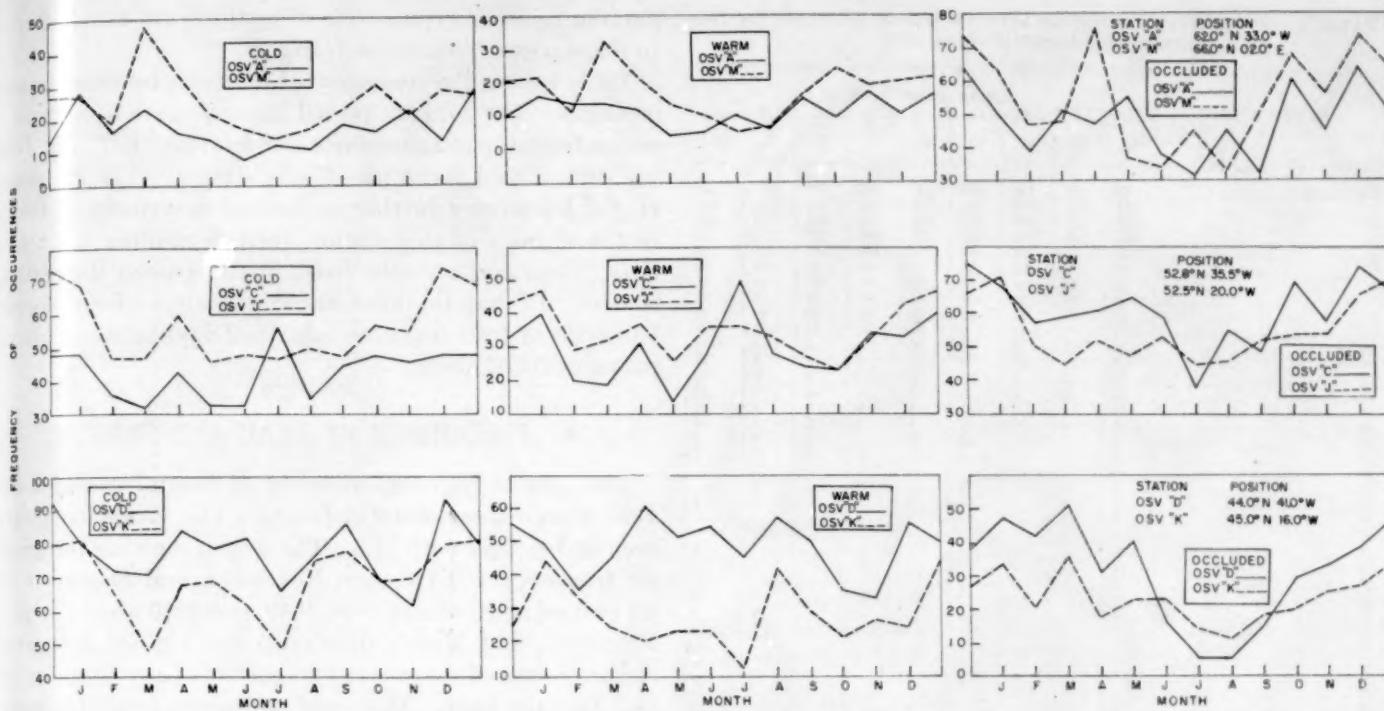


FIGURE 3.—Comparison of frequency of frontal passages at North Atlantic Ocean Station Vessels located in the same latitudinal zone for the period October 1945–June 1957.

affected station's temperature, dew point, pressure, and wind for the day before, the day of, and the day following frontal passage. Summaries of the data are presented in tables 1–4 and figures 2–7. Actual frequencies rather than percentage frequencies are shown so that contrasts between locations may be more sharply delineated.

During the period of 11 years and 9 months, there were 12,295 major frontal passages at the Ocean Station Vessel positions in the North Atlantic, or an average of 116.3 passages per station per year.

TABLE 2.—*Monthly total frequency and average frequency of frontal passages (all types) by station and month for the period October 1945–June 1957*

Stations	January	February	March	April	May	June	July	August	September	October	November	December		
													Month	Frequency
A Total	94	75	91	79	73	54	54	63	70	87	86	88		
Average	8	6	8	7	6	5	5	6	6	7	7	7		
B Total	71	65	61	67	69	76	104	88	105	108	87	73		
Average	6	5	5	6	6	6	10	8	10	9	7	6		
C Total	160	120	113	138	112	120	146	119	121	147	140	158		
Average	13	10	9	12	9	10	13	11	11	12	12	13		
D Total	182	155	174	186	172	160	125	119	159	142	131	195		
Average	15	13	15	16	14	13	11	14	15	12	11	16		
E Total	140	143	163	118	95	55	19	25	60	107	107	140		
Average	12	12	14	10	8	5	2	2	6	9	9	12		
I Total	158	90	125	123	101	97	96	77	93	142	115	145		
Average	13	8	10	10	8	8	9	7	9	12	10	12		
J Total	189	129	131	151	124	140	132	131	129	139	146	184		
Average	16	11	11	13	10	12	12	12	12	12	12	15		
K Total	166	122	112	110	117	113	78	129	128	116	125	137		
Average	14	10	9	9	10	9	7	12	12	10	10	11		
M Total	115	79	132	134	74	66	64	61	92	125	97	123		
Average	10	7	11	11	6	6	6	6	8	10	8	10		

3. FREQUENCY BY STATION

Outbreaks of cold air move farthest south behind cold fronts in the westernmost region of the ocean area. Generally upon reaching the vicinity of the Gulf Stream the southward movement is arrested. The predominant

TABLE 3.—*Extreme frequencies of frontal passages by station and type for the period October 1945–June 1957*

Station	Type	Highest frequency		Lowest frequency	
		Month	Frequency	Month	Frequency
A	Cold	January	28	June	8
	Warm	November	17	May	4
	Occluded	December	64	July	31
B	Cold	September	28	November	14
	Warm	July	30	April	6
	Occluded	October	69	March	33
C	Cold	July	56	March	32
	Warm	July	50	May	14
	Occluded	December	75	July	38
D	Cold	December	93	November	62
	Warm	April	60	November	33
	Occluded	March	51	July, August	5
E	Cold	March	111	July	14
	Warm	February	42	July, August	4
	Occluded	January, Febrary	10	July, August, September	0
I	Cold	January	46	August	16
	Warm	December	34	June, August	10
	Occluded	January, December	78	May	43
J	Cold	December	74	May	46
	Warm	January	47	October	23
	Occluded	January	71	March, July	45
K	Cold	January	81	March	48
	Warm	January	44	July	12
	Occluded	March	36	August	11
M	Cold	March	48	July	14
	Warm	March	32	July	5
	Occluded	April	76	August	33

TABLE 4.—Frequency of intervals between frontal passages for the period October 1945–June 1957

Number of days	Ocean station vessels									
	A	B	C	D	E	I	J	K	M	
Less than 1	70	87	196	329	151	163	250	167	128	
1	217	171	403	591	238	346	504	376	328	
2	164	178	333	423	236	282	377	322	245	
3	124	130	257	273	181	206	229	215	137	
4	79	95	137	157	110	116	145	121	92	
5	49	88	94	88	75	80	80	84	52	
6	37	51	44	63	52	36	53	43	46	
7	30	36	30	24	35	37	24	33	28	
8	23	28	29	12	27	35	20	26	24	
9	21	15	18	5	17	19	17	11	23	
10	14	22	8	4	20	15	9	12	14	
11	9	14	13	5	7	6	11	6	17	
12	11	13	2	3	8	12	8	9	9	
13	10	9	7	3	5	4	6	11	15	
14	6	11	1	3	6	1	6	6	11	
15	4	8	1	1	4	5	3	4	5	
16	3	5		3	2	2	2	4	7	
17	5	5	1			2	2	2	2	
18	6	1	1		4	4		3	1	
19	7	2		1		3		3		
20	3	4	1		1			1	1	
21	4	2				1				
22	6	2				1	3		1	
23	5	1	1			1	2		3	
24	1	2	2		1	2		1	1	
25	5	1	1						5	
26	1				1			1	3	
27	4							1	1	
28							1	1		
29		1								
30	1				1	1				
31					1		1			
32		1				1			1	
33						1				
34		1							1	
35	2		1							
36										
37										
38		1			1				1	
39						1				
40										
41	1	1			2				1	
42					1					
43						1				
44										
45										
46										
47										
48										
49										
50										
51										
52										
53										
54										
55										
56										
57										
58										
59										
60										
61										
62										
63										
64										
65										
66										
67										
68										
69										
70										
71										
72										
73										
74										
75						1				

frontal zone then parallels the northeastward course of the Gulf Stream flow.

Tables 1 and 2 indicate that Station "D" at 44.0° N., 41.0° W. experiences the highest frequency of frontal passages, all types of fronts considered. Schumann and van Rooy [8] also show the greatest frequency in this area of the oceanic region. This station also shows a maximum of 919 cold frontal passages and 569 warm frontal passages (fig. 2). It is situated in about the mean annual position of the polar front in the area where the Labrador current meets the Gulf Stream. Most occluded frontal passages occurred at Station "C," to the northeast at 52.8° N., 35.5° W.

Stations "A" and "B," although having the lowest frequency of total frontal passages (tables 1 and 2), display a feature of the Icelandic Low by their relatively high proportion of occluded frontal passages (fig. 2). Stations "I," "J," and "M" are similarly influenced, while "K," farther to the south, shows a high incidence of cold frontal passages. Station "E," the southernmost station, also has a high proportion of cold frontal passages in com-

parison to other types. These features are also reflected in the extreme frequencies (table 3).

Table 4 gives the frequency of intervals between frontal passages. The longest period on any station without a major frontal passage occurred on Station "E". On June 20, 1951, a cold front passed the station. The Bermuda High blocked any further southward movement of fronts in the vicinity of this station until September 3, 75 days later, when another cold front finally passed the station. Station "D" has the most rapid exchange of air masses. Intervals of from less than 1 day to 2 days between frontal passages are common.

4. FREQUENCY BY YEAR AND SEASON

The year of highest frequency of frontal passages was 1953 with a total of 1,213 fronts. The lowest frequency occurred in 1947 with 845. The season showing the greatest frequency was October, November, and December for all years studied except 1946, 1949, and 1950 when January, February, and March displayed the highest frequency. January showed the greatest frequency of any single month and July the least. Most cold and warm frontal passages occurred in January and most occluded frontal passages in December. The least number of cold and warm fronts occurred in the month of May, while July proved to be the month of fewest occlusions.

Figure 3 compares stations at approximately the same latitude in the eastern and western regions of the Atlantic. The modifying effects of the warm and cold stream circulations on the overlying air are easily seen. Stations "D" and "K" show the greatest contrast in warm frontal passages. At station "K" the Gulf Stream has become so diffused and mixed in its path across the Atlantic that it has now lost most of its identifying characteristics and is itself beginning its southward flow along with the cold air on the eastern part of the Atlantic. A sharp contrast in frequencies of frontal passages at high and low latitude stations is shown in figures 4 and 5. These graphs show the transition of frontal systems due to the effects of the Gulf Stream. Moving northward a great deal of the modified air is caught in the flow around the Icelandic Low.

A frequency distribution of the temperature differences of the day before the frontal passage and the day following for a sample of 6,820 fronts on all stations was computed (fig. 6). Temperature data for cold, warm, occluded, and stationary fronts were combined for this study. Temperature of the air was modified so rapidly that the mean 48-hour temperature change was near zero. In other words, on the average the temperature at 1230 GMT the day following the frontal passage had returned to about the same value as that of the day before the frontal passage. (In contrast, at land stations the day following a frontal passage usually provides extreme temperatures.) The standard deviation of the distribution is 4.6°F. and out of the

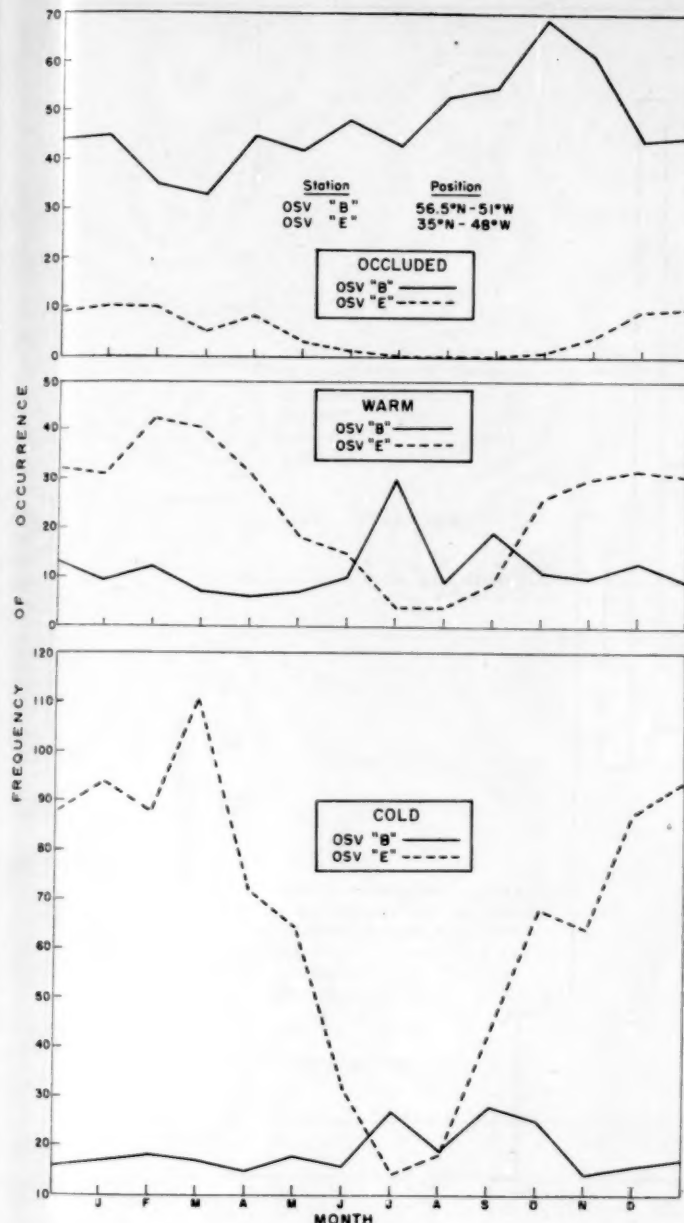


FIGURE 4.—Comparison of frequency of frontal passages at western-most North Atlantic Ocean Station Vessels at high and low latitude for the period October 1945–June 1957.

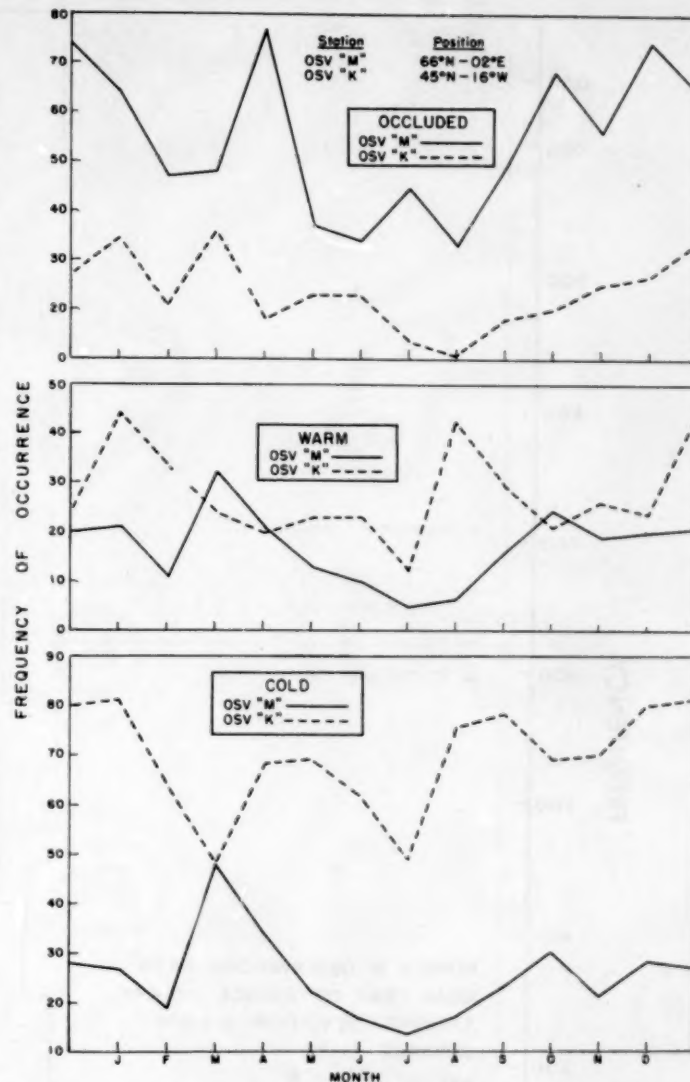


FIGURE 5.—Comparison of frequency of frontal passages at eastern-most North Atlantic Ocean Station Vessels at high and low latitude for the period October 1945–June 1957.

though situated in the Labrador Current, demonstrate the profound and far-reaching influence of the Gulf Stream.

5. CONCLUDING REMARKS

This paper has presented a few basic statistics on frontal passages over an ocean area frequently traversed by both ships and aircraft. The data were compiled from synoptic weather maps, which are used rather infrequently as a source for climatological summarization.

This effort has demonstrated the degree of facility with which historical sea level synoptic maps may be used to determine a preliminary climatology of well-known features of atmospheric motion systems. It is hoped that it will direct some further thinking toward a useful climatology of dynamic systems in the general circulation.

sample of 6,820 frontal occurrences 5,049 of the 48-hour temperature changes fall within one standard deviation from the mean and 6,422 within two standard deviations. This indicates the effectiveness of the heat storage in the oceans in contrast to shallow heating and quick loss of heat by land masses. The same general results would be obtained with any single frontal type. Figure 7 gives a comparison of Stations "A" on the east of the southern tip of Greenland and "B" on the west against the most southern station, "E". Both of the northern stations, even

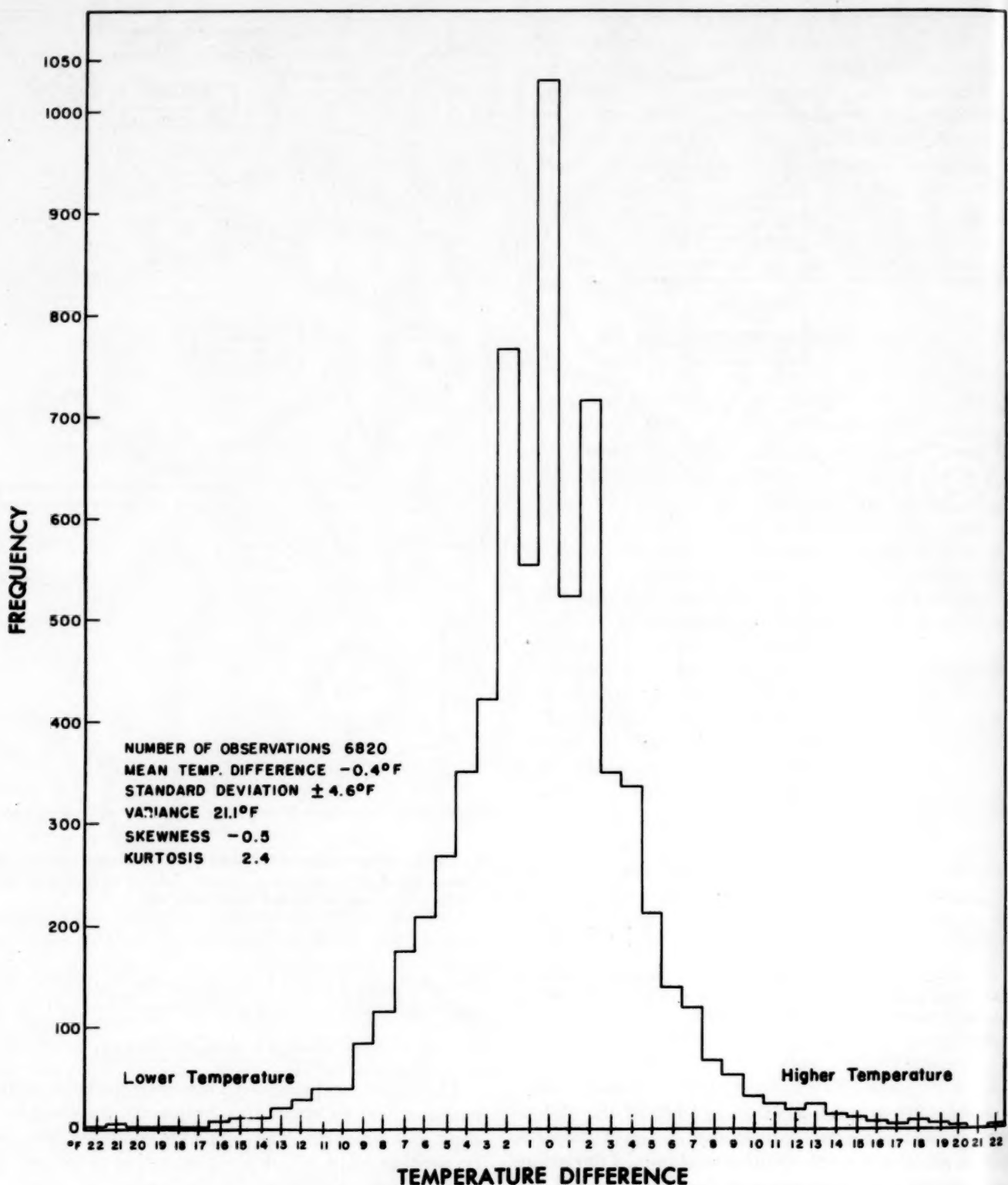


FIGURE 6.—Frequency of 48-hour temperature changes from 1230 GMT on day before to 1230 GMT on day after frontal passage for all North Atlantic Ocean Station Vessels. Temperature data for cold, warm, occluded, and stationary fronts are combined for all stations for the period October 1945–June 1957.

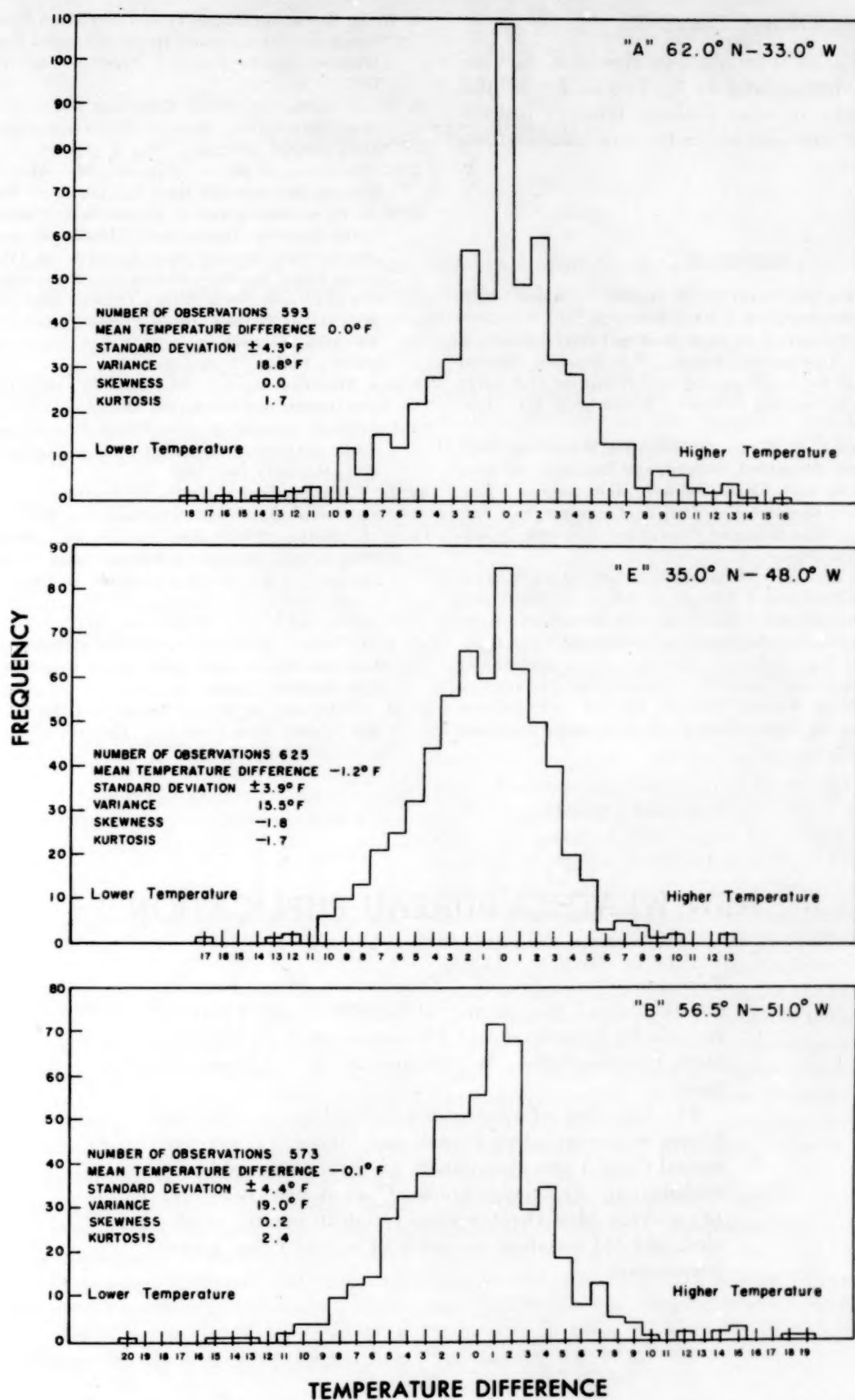


FIGURE 7.—Frequency of 48-hour temperature changes from 1230 GMT on day before to 1230 GMT on day after frontal passage at North Atlantic Ocean Station Vessels "A," "B," and "E." Temperature data for cold, warm, occluded, and stationary fronts are combined for the period October 1945–June 1957.

ACKNOWLEDGMENTS

Sincere appreciation is extended to Messrs. N. L. Canfield, W. M. McMurray, and L. E. Truppi for helpful suggestions and also to other National Weather Records Center personnel who assisted with data compilations, drafting, and typing.

REFERENCES

1. J. Bjerknes, "On the Structure of Moving Cyclones," *Geophysiske Publikasjoner*, vol. 1, No. 2, 1919, 8 pp.
2. R. C. Gentry, "Formation of New Moving Centers South of Deep Lows," (Preliminary Report) U.S. Weather Bureau Research Paper No. 7, (Contained in *A Collection of Reports on Extended Forecasting Research*) Washington, D.C., Jan. 1944.
3. R. C. Gentry and L. L. Weiss, "Preliminary Report on Stagnant Highs over Greenland, Iceland, and England, and over the Bering Sea and Alaska in July and August," U.S. Weather Bureau Research Paper No. 9, (Contained in *A Collection of Reports on Extended Forecasting Research*) Washington, D.C., Jan. 1944.
4. Z. Gregor and L. Krivsky, "Mnogoletnee Izmenenie Tsirkulatsii Atlanticheskogo-Evropeiskoi Oblasti v Sviazi s Sekularnoi Solnechnoi Deiatel'nosti," [Long-Period Fluctuations of the Circulation in the Atlantic-European Region and Their Relation to Secular Solar Activity], Czechoslovakian Academy of Sciences, Geophysical Institute, *Transactions (Geophysics Collection)* No. 62, Prague, 1957, pp. 165-215. (Translated 1958 by American Meteorological Society under Contract AF19(604)-1936.)
5. W. H. Klein, "Principal Tracks and Mean Frequencies of Cyclones and Anticyclones in the Northern Hemisphere," U.S. Weather Bureau Research Paper No. 40, Washington, D.C. 1957.
6. W. M. McMurray, "Data Collection for the Northern Hemisphere Map Series," *Monthly Weather Review*, vol. 84, No. 6, June 1956, pp. 219-234.
7. S. Petterssen, *Weather Analysis and Forecasting*, vol. 1, 2d Edition, McGraw-Hill Book Co., Inc., New York, 1956.
8. T. E. W. Schumann and M. P. van Rooy, "Frequency of Fronts in the Northern Hemisphere," *Archiv für Meteorologie, Geophysik, und Bioklimatologie, Series A*, vol. IV, 1951, pp. 87-97.
9. U.S. Air Force, *Northern Hemisphere Historical Weather Maps, Sea Level and 500 Millibars*, October 1945-December 1948.
10. U.S. Weather Bureau, *Daily Series Synoptic Weather Maps, Northern Hemisphere, Part I, Sea Level and 500 Millibar Charts*, January 1949-June 1957.
11. U.S. Weather Bureau, *Historical Weather Maps, Northern Hemisphere, Sea Level*, 1899-1939.
12. U.S. Navy, Bureau of Aeronautics, Project AROWA, "Climatology of Ocean Cyclones," Technical Report Task 13, (TED-UNL-MA-501), Dec. 1952.
13. L. L. Weiss, Long Range Forecasting "Aid", Unpublished manuscript U.S. Weather Bureau, Dec. 1945.
14. L. L. Weiss, "Preliminary Report on Duration of Stormy Periods at Selected Localities and Intervals Between Periods," U.S. Weather Bureau Research Paper No. 3 (Contained in *A Collection of Reports on Extended Forecasting Research*), Washington, D.C., Jan. 1944.
15. L. L. Weiss, Some Characteristic Meteorological Conditions from the Historical Weather Maps, Unpublished manuscript, U.S. Weather Bureau, ca. 1945.
16. H. Wexler and M. Tepper, "Results of the Wartime Historical and Normal Map Program," *Bulletin of the American Meteorological Society*, vol. 28, No. 4, Apr. 1947, pp. 175-178.

NEW WEATHER BUREAU PUBLICATION

Technical Paper No. 37, "Evaporation Maps for the United States," Washington, D.C., 1959, 13 pp., 5 plates; for sale by Superintendent of Documents, U.S. Government Printing Office, Washington 25, D.C. Price, 65 cents.

The following information is presented by chart for the United States excluding Hawaii and Alaska: (1) average annual Class A pan evaporation, (2) average annual lake evaporation, (3) average annual Class A pan coefficient, (4) average May-October evaporation in percent of annual, and (5) standard deviation of annual Class A pan evaporation.

CORRESPONDENCE

Comments on "Power Spectrum Analysis of Climatological Data for Woodstock College, Maryland"

J. K. ANGELL

U.S. Weather Bureau, Washington, D.C.

November 20, 1959

In their article in the August 1959 issue of the *Monthly Weather Review*, Landsberg, Mitchell, and Crutcher [1] mention the predominant periodicity found in transsonde-derived winds (50-hour period) as supporting evidence for a 3-day Eulerian periodicity found from precipitation records at Woodstock College, Maryland. One must be careful in comparing Lagrangian and Eulerian periodicities since the time it takes for the transsonde at 300 mb. to pass through a long wave in the westerlies may have little correspondence to the time it takes this long wave to pass over a surface station. Therefore, some calculations are in order.

If these long waves move with a speed c of 18° longitude per day (34 knots at latitude 40°), as suggested by the authors, then, since the average zonal component of the wind speed \bar{u} at latitude 40° along the transsonde trajectories is about 80 knots, the average trajectory wavelength L is 4,000 nautical miles, and since

$$L_s = (\bar{u} - c)L/\bar{u}, \quad (1)$$

where L_s is the streamline wavelength, we find from substitution of the above values

$$L_s = \frac{(80 - 34)}{80} \times 4000 = 2300 \text{ nautical miles.} \quad (2)$$

Interestingly enough, a long wave moving at a speed of 34 knots with the above streamline wavelength would pass over a surface station in 68 hours. Thus, if the long waves actually move with a speed of 34 knots in the average, the transsonde-derived wind fluctuations tend to support the 3-day periodicity in precipitation. However, if the average wave speed is assumed to be only two-thirds of 34 knots (which seems more reasonable to this writer), then the streamline wavelength deduced from the predominant transsonde periodicity is about 2,900 nautical miles and the wave would pass over the station in 128 hours. Thus, if the long waves move with a speed of about 22 knots in the average, the transsonde-derived wind fluctuations

tend to support the 5- to 7-day periodicity found in precipitation records at Woodstock College. Obviously, the results are very sensitive to the value chosen for the long-wave speed and for this reason it would be desirable to evaluate as carefully as possible the average value for this long-wave speed before suggesting that the transsonde wind fluctuations are associated with one or the other of the precipitation periodicities.

REFERENCE

1. H. E. Landsberg, J. M. Mitchell, Jr., and H. L. Crutcher, "Power Spectrum Analysis of Climatological Data for Woodstock College, Maryland," *Monthly Weather Review*, vol. 87, No. 8, Aug. 1959, pp. 283-298.

Reply

H. E. LANDSBERG, J. M. MITCHELL, JR., AND H. L. CRUTCHER
Office of Climatology, U.S. Weather Bureau, Washington, D.C.

December 16, 1959

We are grateful to Dr. Angell for his very cogent comments on our paper. We are, of course, aware of the pitfalls of comparing Eulerian and Lagrangian periodicities.

We hope that it is obvious from our text as well as from the varying periodicities shown for different discrete time intervals on figures 1 and 2 that we were not too concerned with very specific values for the length of a given periodicity but rather with the fact that for certain intervals of time such periodicities in the 3- to 10-day range exist in the atmosphere. It was quite clear to us that use of local observations of precipitation is not the best approach to get at these fluctuations and that other more representative parameters of short periodic atmospheric fluctuations could and should be used for further investigations. The really important target of these investigations should be the determination of the causes for periodicities of this length and when and why changes occur from one preferred period to another.

This also gives us a welcome opportunity to correct some misprints which were overlooked in proofreading. On page 284, column 1, line 26, the word "infinitesimally" should read "infinitely" and on page 293, column 1, bottom line, "equation (3)" should read "equation (13)". On page 295, in table 2, harmonic 18, the inclusive period should read "4.9 to 5.2."

THE WEATHER AND CIRCULATION OF NOVEMBER 1959

Unusually High Persistence From October

JAMES F. ANDREWS

Extended Forecast Section, U.S. Weather Bureau, Washington, D.C.

1. HIGHLIGHTS

The outstanding feature of November 1959 was the marked persistence of both circulation and weather from October 1959. Subnormal temperatures continued to dominate most of the United States,¹ with a period near mid-month of unusual cold from the Middle and Upper Mississippi Valley to the Pacific Northwest. The coldest weather was centered in Montana, where long-period temperature and precipitation records were broken. The cold wave was quickly followed by rapid warming and a circulation reversal which heralded a change in regime during the latter part of the month. Other highlights of November were the continued lack of rainfall in much of California and Nevada, record snowfall in Montana, and heavy rains in southern Florida.

2. PERSISTENCE FROM OCTOBER

The circulation pattern at 700 mb., over the Pacific and North America was extremely persistent from October to November 1959. This is apparent from a comparison of the 700-mb. mean contours and anomaly patterns for November (figs. 1 and 2) with those for October (figs. 1 and 2 of [1]). Over a grid extending from 30° to 50° N. and from 70° to 130° W., the lag correlation between the October and November patterns of height anomaly was +0.87. This is considerably higher than the 1933-59 average (-0.02) and the highest ever observed for this 27-year period.

The temperature and precipitation patterns over the United States were also highly persistent from October to November 1959. In table 1 are shown the class changes of monthly mean temperature and total precipitation for an array of 100 fairly evenly distributed stations. With respect to temperature, the classes much above and much below normally occur 12½ percent of the time each, and above, normal, and below normally occur 25 percent of the time each. Persistence of temperature may be considered in terms of the total zero-plus-one class change

TABLE 1.—*Class changes of weather anomalies in the United States from October to November 1959*

Temperature		Precipitation	
Class change	Frequency (%)	Class change	Frequency (%)
0	33	0	46
1	52	1	28
2	14	2	16
3	1		
4	0		

[2]. From October to November 1959, 85 percent of the country did not change by more than one class. This is well above the average of 61 percent for the period 1942-1959.

Precipitation is divided into three classes, each normally occurring 33⅓ percent of the time, and persistence generally refers to zero class changes only [2]. From table 1, it is seen that 46 percent of the country remained in the same precipitation class from October to November 1959. This is the second highest precipitation persistence observed during the period 1942-59 and well above the average of 34 percent for the same period.

3. MONTHLY MEAN CIRCULATION

The average circulation pattern at 700 mb. for November 1959 (fig. 1) was of a relatively simple sinusoidal type with well defined trough-ridge systems close to their normal positions [3]. This circulation was remarkably similar to October's circulation, not only over North America as mentioned in the previous section, but also over eastern Asia and the Pacific. This is evident from the small anomalous height changes between the two months (fig. 2). The greatest change in circulation occurred over Russia, where 700-mb. heights rose as much as 610 feet as a deep trough at middle and high latitudes was replaced by a strong ridge. A change of lesser magnitude in the Atlantic was associated with replacement of rather flat cyclonic flow by a slightly stronger than normal ridge (fig. 1).

Blocking during November was centered primarily in higher latitudes where 700-mb. heights were above normal

¹United States as used in this paper does not include Alaska and Hawaii.

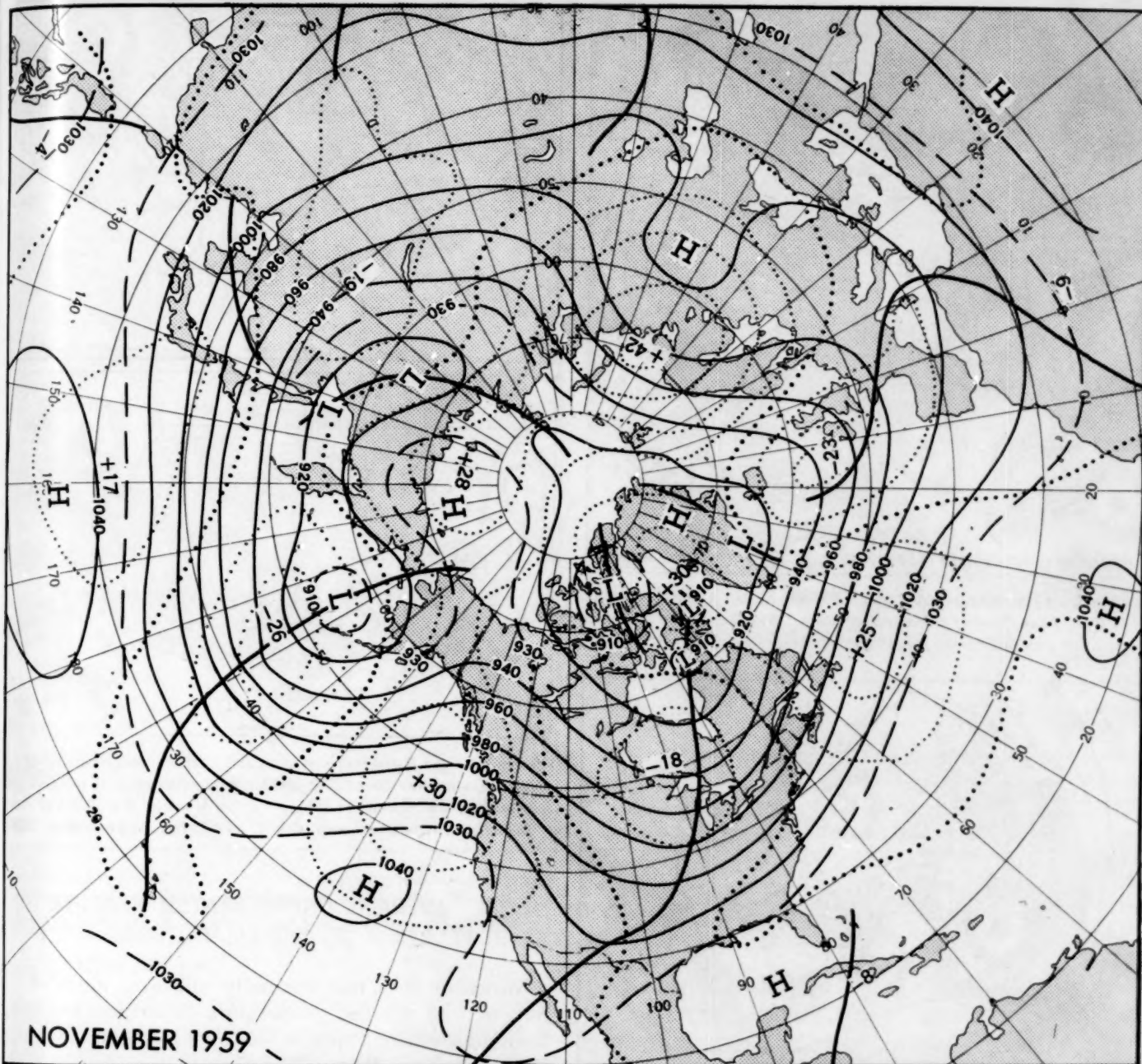


FIGURE 1.—Mean 700-mb. contours (solid) and height departures from normal (dotted) (both in tens of feet) for November 1959. Principal features affecting United States weather were the strong ridge along the west coast of North America and the deep trough in mid-continent.

north of 70° N. (fig. 1). The strong blocking High centered over the Bering Sea and Kamchatka Peninsula during October [1] weakened as it moved northwestward, and in November it was centered over the Arctic basin. Relaxation of this block allowed the Aleutian Low to deepen and move northward from its October position. Weak blocking appeared in North America in the form of an area of positive height anomaly centered over Davis Strait. The strongest blocking affected Europe and Russia and was

associated with an extensive area of positive height anomaly centered over the Barents Sea (fig. 1).

The principal axis of maximum west wind at 700 mb. appeared as a well defined jet extending around nearly the entire Northern Hemisphere (fig. 3). Over Europe this jet separated into two branches in association with the block affecting that region. The southern branch was related to a storm track located farther south than usual and with consequent increased storminess in the Mediter-

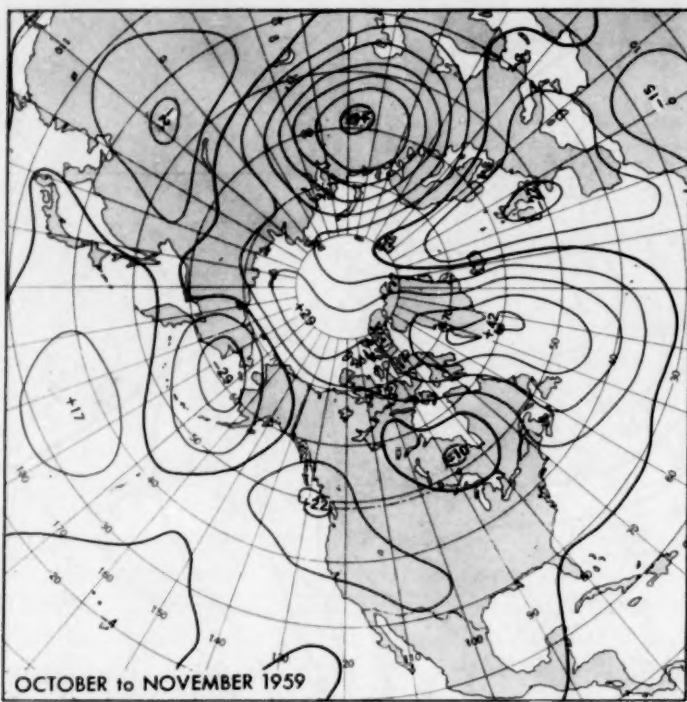


FIGURE 2.—Change in monthly mean 700-mb. height anomalies (tens of feet) from October to November 1959. Small changes in North America and the Pacific reflect great persistence of the circulation.

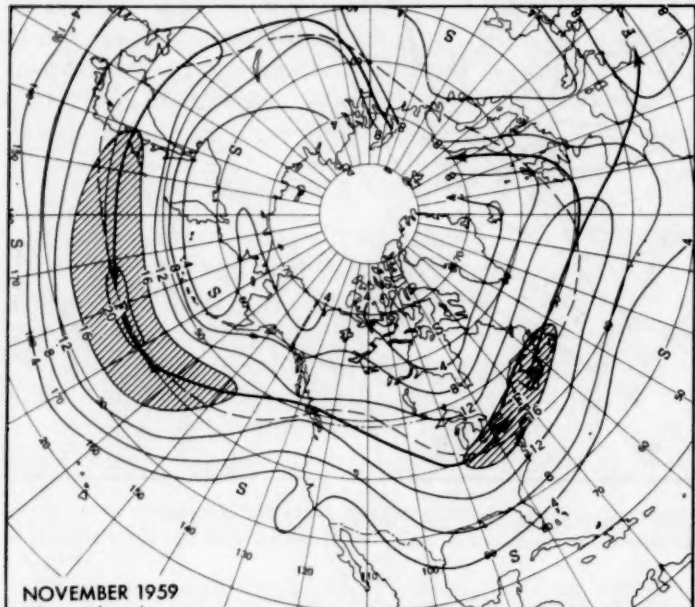


FIGURE 3.—Mean 700-mb. isotachs (meters per second) for November 1959. Solid arrows indicate position of the principal jet axis, which was close to its normal position (dashed) over the entire Northern Hemisphere. "F" and "S" show centers of fast and slow wind speeds respectively. Areas of wind speed greater than 16 m.p.s. are hatched.

ranean and southern Europe during November. Wind speeds in the primary jet were strongest over the mid-Pacific and New England but mostly subnormal over the southern portion of the Atlantic, most of Europe, and central Asia.

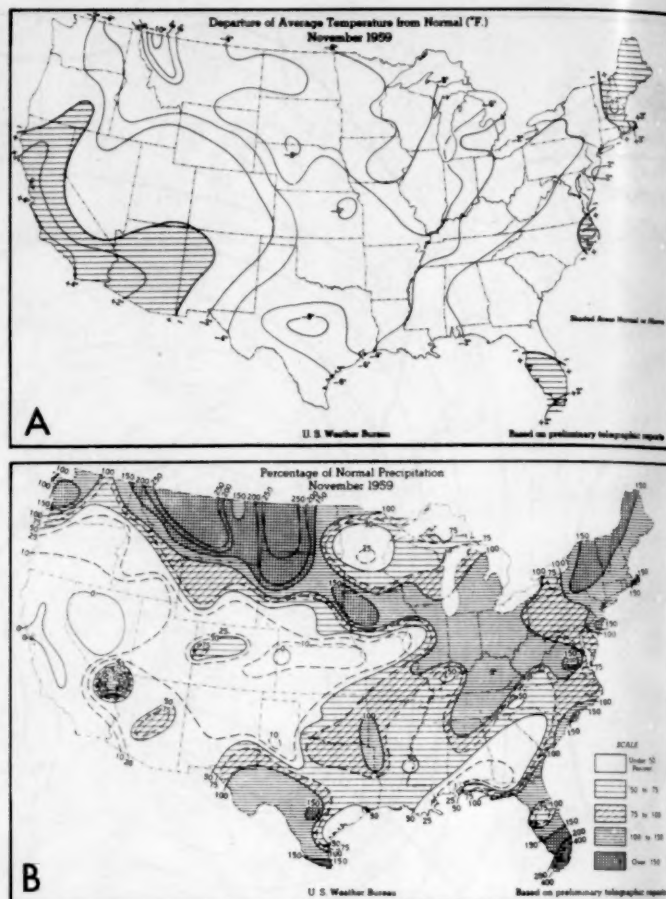


FIGURE 4.—(A) Departure of average surface temperature ($^{\circ}$ F.) from normal for November 1959, (B) Percentage of normal precipitation for November 1959. (From *Weekly Weather and Crop Bulletin, National Summary*, vol. XLVI, No. 49, December 1959.)

4. AVERAGE UNITED STATES WEATHER IN RELATION TO THE MEAN CIRCULATION

November 1959 was unusually cold over much of the Nation, with greatest temperature departures extending from the southern Plains to the Great Lakes and westward to the northern Rocky Mountain States (fig. 4A). In many areas from Texas to the western Great Lakes this was the coldest November of record. The greatest departure was observed at International Falls, Minn., where the average temperature for the month was 10° F. below normal. The most extreme cold was experienced in Montana and will be discussed in the following section. Temperatures of -22° F. at Valentine, Nebr. and -19° F. at Rapid City, S. Dak. on the 14th were record November minima, while at Sheridan, Wyo. it was -25° F. on the 16th, the second lowest temperature ever recorded in November. Many daily minimum temperature records, too numerous to mention, were established throughout the Nation. From Texas northeastward the coldest weather was generally experienced on the 17th and 18th, when many stations reported their lowest temperatures ever observed so early in

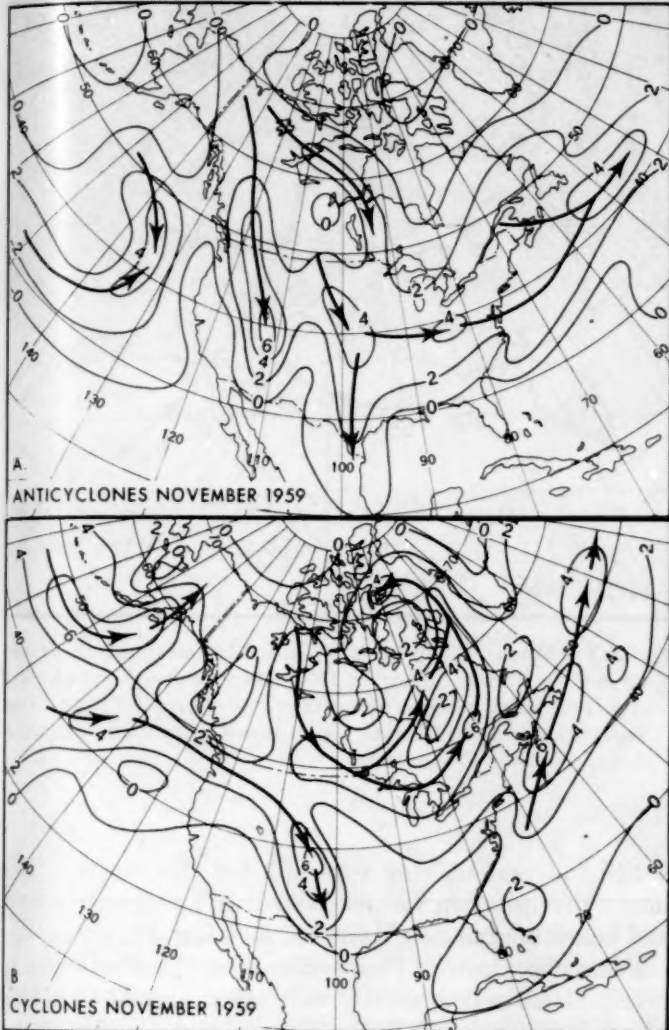


FIGURE 5.—Frequency of (A) anticyclone passages and (B) cyclone passages (within equal area boxes of 66,000 n. mi.²) during November 1959. Primary tracks are indicated by solid arrows.

the season. This cold was associated with a strong Arctic high pressure area which brought a sea level pressure of 30.84 inches to Dallas, Tex., on the 17th, a new November record.

The unseasonable cold was associated with stronger than normal northerly flow between the strong ridge along the west coast of North America and the deep trough over the mid-continent (fig. 1). Sea level pressures averaged as much as 8 mb. above normal in British Columbia (see chart XI in [4]), while there were two primary anticyclone tracks associated with the cold polar outbreaks, one on either side of the Continental Divide (fig. 5A). Northwesterly flow aloft over the Rockies tended to contain the coldest weather east of the Divide (figs. 1, 4A). The mean monthly thickness of the layer between 1000 mb. and 700 mb. was also abnormally cold over much of North America, with greatest departures centered over Manitoba (fig. 6).

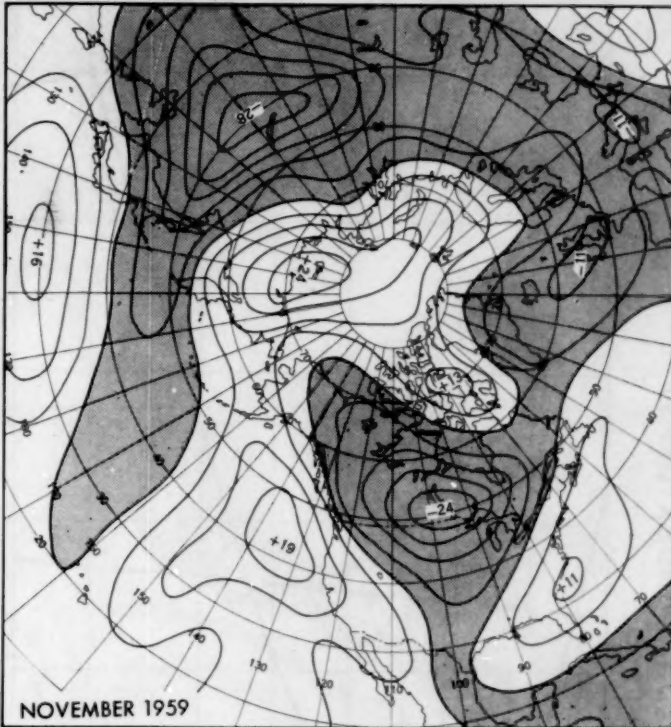


FIGURE 6.—Mean 1000-700-mb. thickness departure from normal (in tens of feet) for November 1959, with areas of subnormal values shaded. Abnormally cold air covered much of North America.

Most of California continued to observe above normal temperatures. This was the warmest November at San Diego during a period of record dating to 1872. Blue Canyon had its warmest November in 59 years of record. Bakersfield (83° F.) and Fresno (78° F.) reported record high temperatures for so late in the season on the 27th. At Los Angeles the average daily temperature was 1° F. below normal on the 4th, the first day the temperature had been below normal since February 22, 1959. The California warmth was related to the strong mean ridge along the coast (fig. 1). In addition easterly anomalous flow resulted in frequent Santa Ana winds.

November's precipitation pattern (fig. 4B) is not too difficult to relate to the mean circulation. In general, the heaviest amounts fell near or just to the north of the primary jet axis at 700 mb. (fig. 3). More than twice the normal amount of precipitation occurred in portions of Montana, the Dakotas, and Iowa (fig. 4B). Much of this was in the form of snow and resulted in record or near record depths for the month of November. Disturbances entering the Pacific Northwest and following a primary track southeastward along the Divide (fig. 5B) contributed most of this precipitation. A second storm track along the Canadian border produced lesser amounts in the Northern Plains States and Upper Mississippi Valley.

Much of the precipitation in the East was related to the deep trough in the central United States (fig. 1, 4B). The Northeast was generally wet and cloudy with less

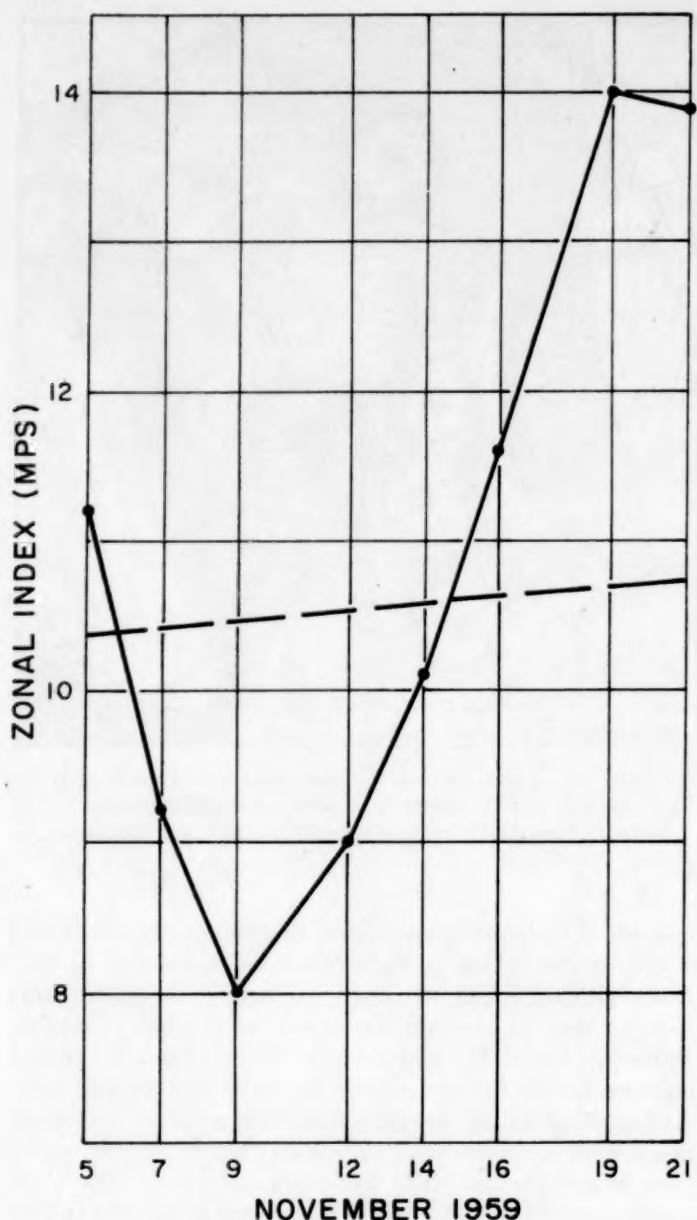


FIGURE 7.—Time variation of speed of 700-mb. westerlies averaged over North America and the Pacific between latitudes 35° and 55° N. and longitudes 65° W. and 175° E. Solid line connects 5-day mean zonal index values (plotted at middle of period and computed thrice weekly), while dashed line gives the corresponding normal. Severe weather changes accompanied the pronounced index cycle.

sunshine than normal as a result of stronger than normal southerly flow at sea level (chart XI in [4]) and aloft (fig. 1). In portions of the Southeast less than half the normal amount of precipitation fell during November (fig. 4B). This was related to the lack of cyclone passages (fig. 5B) and to the weak ridge of positive anomaly at 700 mb. (fig. 1). Rainfall in southern Florida was well above the normal, with Miami receiving 13.15 inches, a new November record. Of this, 7.93 inches fell during

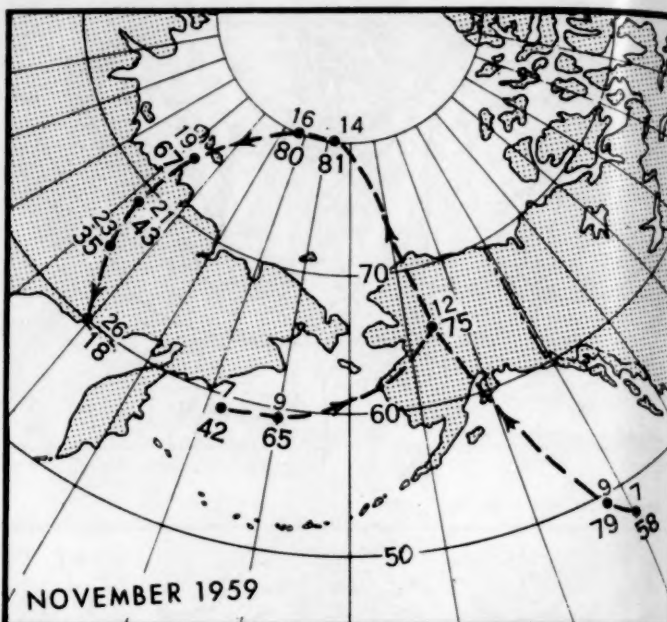


FIGURE 8.—Tracks of important 700-mb. 5-day mean positive anomaly centers during November 1959. Top number is middle day of period; lower number, intensity of center (tens of feet). Coalescence of anomaly centers accompanied pronounced amplification of the circulation pattern.

a 24-hour period, also a record for the month. This heavy precipitation was associated with an easterly wave and below normal heights at 700 mb. (fig. 1).

From the Central Plains States to the Pacific coast, precipitation was generally well below normal (fig. 4B). Many areas, principally in Nevada and California, reported no precipitation at all. This was the first November since 1929 without rain at San Francisco, Calif., and, at month's end, 73 consecutive days had passed without any measurable precipitation there. The moisture deficiency in the West was associated primarily with stronger than normal northerly anticyclonic circulation at 700 mb. (fig. 1).

5. INTRAMONTHLY VARIABILITY IN WEATHER AND CIRCULATION

An extreme change in weather and circulation associated with an index cycle (fig. 7) occurred near mid-month. This pronounced change apparently had its origin in the Pacific, where, during the first week of November, the mean circulation consisted of a trough in the middle flanked by ridges. The western ridge, which extended to the Kamchatka Peninsula, strengthened as it moved slowly eastward and developed a closed anticyclonic circulation at the 700-mb. level over the Bering Sea. At the same time the Aleutian Low was displaced well to the south and, as the pattern amplified, a strong cold air injection accompanied intense cyclogenesis at lower lati-

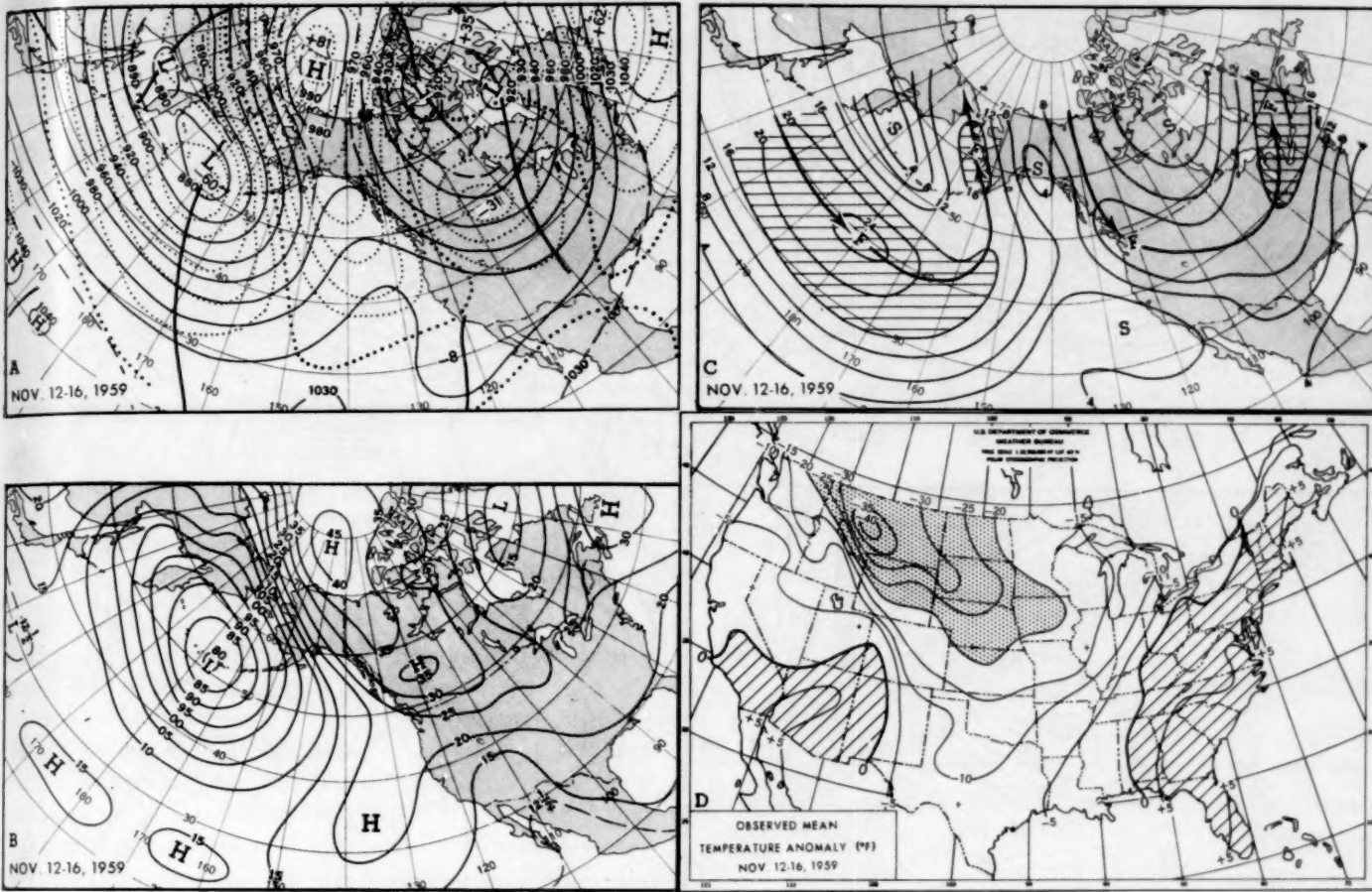


FIGURE 9.—Five-day mean charts for November 12–16, 1959. (A) 700-mb. contours (solid) and height departures from normal (dotted) (both in tens of feet). (B) Sea level isobars (millibars, hundreds omitted). (C) 700-mb. isotachs (meters per second). Solid arrows indicate primary axes of westerly jet; areas with speeds greater than 16 m.p.s. are hatched. (D) Departure of average surface temperature from normal ($^{\circ}$ F.); areas with averages more than 20° below normal are stippled. Areas of above normal temperatures are hatched.

tudes in the mid-Pacific. Sea level pressures in this storm were as low as 980 mb. on the 9th and 10th.

The eastern Pacific ridge quickly responded to these developments and built northward, eventually amalgamating over Alaska with the eastward-moving ridge from the Bering Sea. Tracks and intensities of the accompanying 5-day mean 700-mb. height anomaly centers are shown in figure 8. As northward motion continued, an intense block developed over the Arctic Basin, where heights were as much as 810 feet above normal for the period November 12–16, 1959. In figure 9 are shown the corresponding 5-day mean circulation patterns of 700-mb. height, sea level isobars, 700-mb. isotachs with primary jets, and departure of average surface temperature from normal in the United States. The meridional character of the circulation during this period of low zonal index (fig. 7) is strongly evident. Note also the deep Aleutian Low, displaced southwest of its normal position [3], and the strong polar anticyclone centered over the Arctic.

The strong northerly flow thus created in western Canada deployed extremely cold Arctic air masses south-

ward into the northwestern and middle parts of the United States. Moreover, these air masses remained cold since the flow was cyclonic, thus inhibiting subsidence. Temperatures for the period November 12–16, 1959, averaged as much as 40° F. below normal in Montana (fig. 9D). Helena bore the brunt of the bitter weather, reporting a temperature of -39° F. on the 16th, the lowest temperature ever observed there in November. The average temperature on this day was -24° F., 55° F. below the normal. Local blizzard conditions accompanied the frigid weather, with heaviest snowfall in Montana. Most of that State's November precipitation fell as snow, nearly all of it during the period of severe cold. The total snowfall at Helena was 33 inches, breaking an 80-year November record. A snowfall of nearly 22 inches on the 11th and 12th at the same city was the largest for 24 hours for any month.

As the Arctic air swept southward into Texas and eastward to the Great Lakes, it brought new record low temperatures for so early in the season to many stations in the mid-United States, breaking some records for early season cold established in the 1880's. Temperatures dropped as

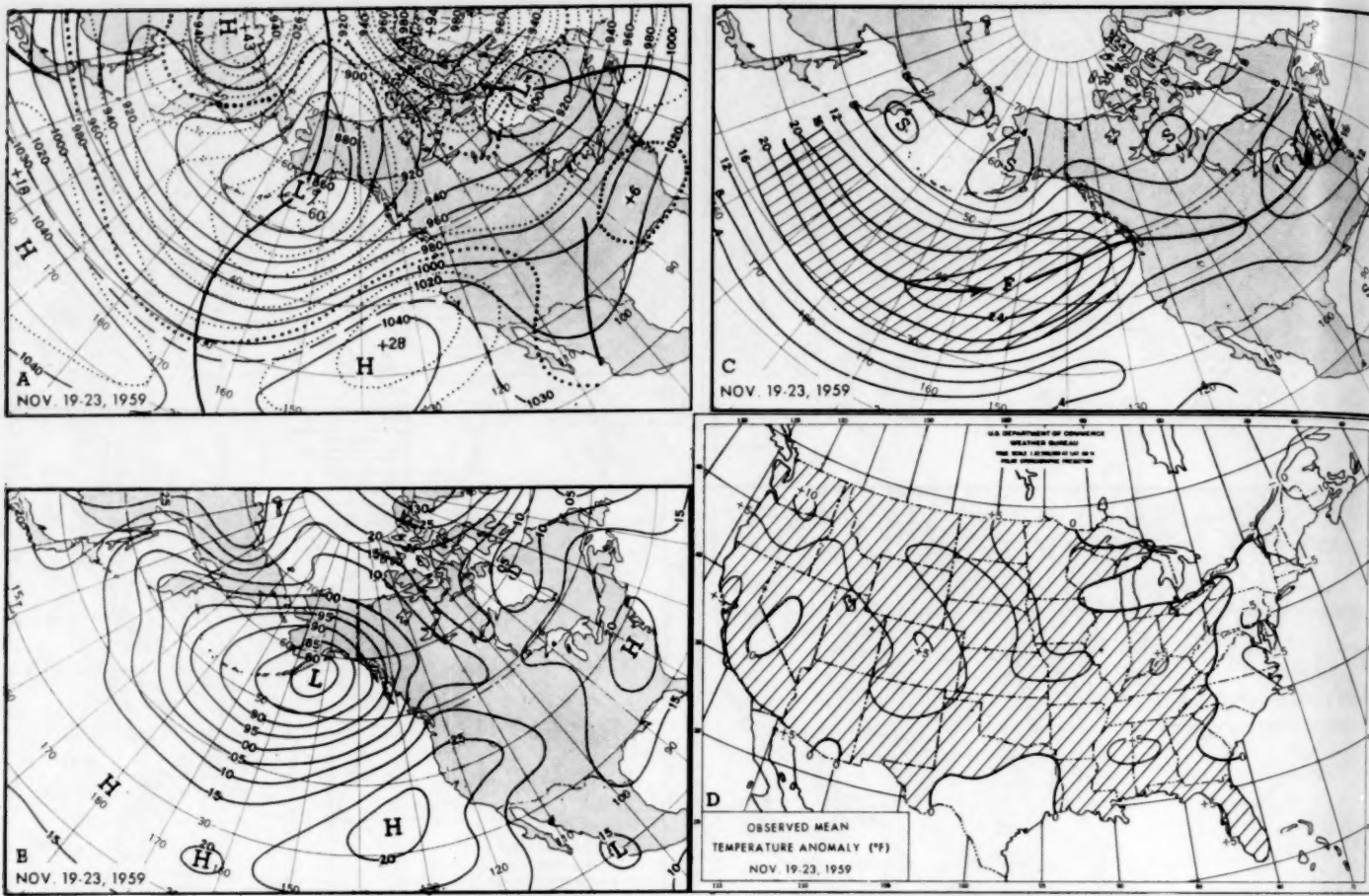


FIGURE 10.—Five-day mean charts for November 19–23, 1959. (A) 700-mb. contours (solid) and height departures from normal (dotted) (both in tens of feet). (B) Sea level isobars (millibars, hundreds omitted). (C) 700-mb. isotachs (meters per second). Solid arrows indicate primary axes of westerly jet; areas with speeds greater than 16 m.p.s. are hatched. (D) Departure of average surface temperature from normal ($^{\circ}$ F.), with areas of above normal hatched.

much as 60° F. over the Great Plains States within 24 hours, with below zero readings extending eastward to Wisconsin and southward to northern Kansas. Some of the Arctic air spilled over the mountains into the Pacific Northwest and the northern Great Basin, bringing mostly cold and clear weather to these areas.

It is of interest to point out that the greatest negative temperature anomalies were contained north of the primary jet axis (figs. 9C, 9D). Furthermore, the period of extreme cold from the 12th to 16th occurred after the zonal index had reached its minimum (Nov. 7–11) and during the ensuing period of rapid recovery (fig. 7). This tendency to have the most severe cold just after index minima was noted early in extended forecasting practice.

During the following week (Nov. 19–23, 1959, fig. 10) the rapid increase in westerlies over the Pacific and North America was associated with a marked reversal in circulation and weather over most of the United States. Retrogression and gradual weakening of the polar block allowed the deep Aleutian Low to move northeastward to its more normal position (figs. 10A, 10B). The motion of these

two centers of action combined to produce a rapid decrease in amplitude and eastward motion of the eastern Pacific ridge, along with a marked increase in the strength of the westerlies. This increase in westerly momentum spread across North America as the mean 700-mb. jet axis was displaced northward west of the Mississippi Valley (fig. 10C) and effectively contained the cold Canadian air masses.

Much warmer weather accompanied this change in mid-tropospheric circulation, with above normal temperatures observed in the area where one week before they averaged far below normal (figs. 9D, 10D). Figure 11 shows that the greatest increase in average temperature between the two 5-day periods was 49° F. at Helena, Mont.

Strong westerly winds brought rapid warming and very heavy rains over the western slopes of the Cascades and along the coast to central Oregon. A temperature of 69° F. at Yakima, Wash., on the 23d, established a record for so late in the season. As much as 6 inches of rain fell locally in 24 hours, with the amounts at Seattle and Olympia, Wash., setting November records. Serious

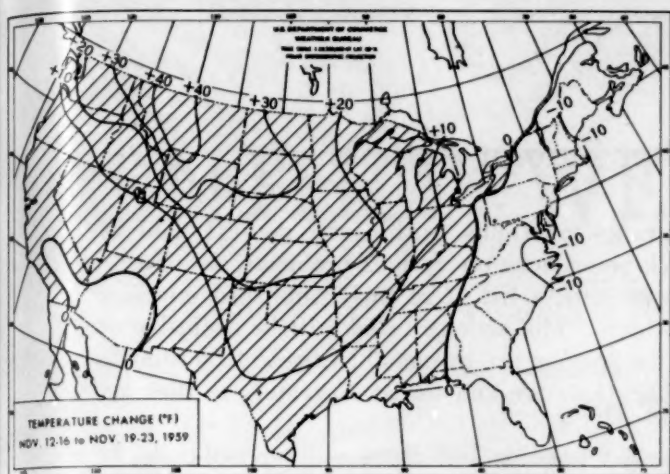


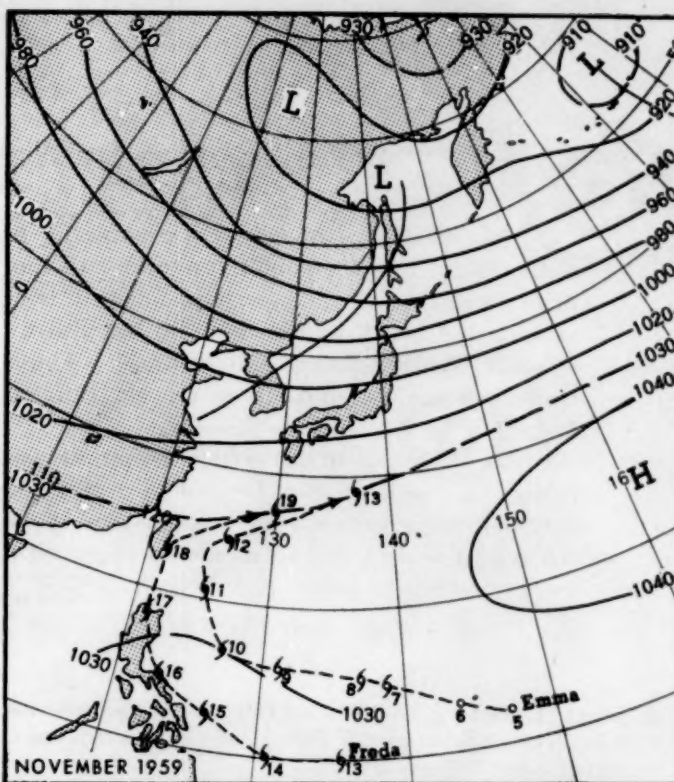
FIGURE 11.—Change in 5-day mean surface temperature anomalies ($^{\circ}$ F.) from November 12-16 to November 19-23, 1959. Hatched areas represent a change to warmer.

flooding occurred along the Green, Snoqualmie, and Snohomish Rivers in Washington as alltime high flood stages were recorded.

Major reversals in weather and circulation of the type described above are not particularly uncommon. Saylor and Caporaso [5], using daily synoptic charts, found that similar abrupt changes of this type occurred nearly every November, often heralding the onset of winter in the central United States. This year, however, persistent cold was gradually replaced by a warm regime.

6. PACIFIC TYPHOONS

Tropical storm activity during November was confined primarily to the Pacific, where two typhoons were observed. Tracks of these storms, Emma and Freda, superimposed on the mean 700-mb. contours for the month, are shown in figure 12. Both storms recurved in the usual area of recurvature. After recurvature, however, neither assumed the characteristics of a deep extratropical storm, but instead both were swept rapidly eastward as weak disturbances. This lack of development was probably associated in part with the stronger than normal ridge in the western Pacific (fig. 1).



Publications by Weather Bureau Authors

The Weather Bureau's work covers a wide range of topics within the general field of meteorology. To acquaint the public with the work being done on various problems, we plan to print from time to time, perhaps monthly if space permits, a list of recently published scientific articles and books written by Weather Bureau authors. The articles listed will be exclusive of those in Weather Bureau publications. (Those in the *Review* are presumably already familiar to readers of the list, and other Weather Bureau publications are announced separately as they are issued.)

We shall try to make the listing as complete as possible but there will undoubtedly be omissions, which we shall be glad to rectify when brought to our attention. Since the first several lists will cover papers from the last year or two, we will make each list a random selection from the complete alphabet so as not to slight either the A's or the Z's. Subsequent lists should be more closely up to date.

- J. K. Angell, "Estimating the Frictional Force at 300 mb. by Means of Transsonde and Radiosonde Data," *Journal of Meteorology*, vol. 16, No. 2, Apr. 1959, pp. 216-217.
- E. M. Ballenzweig, "Relation of Long-Period Circulation Anomalies to Tropical Storm Formation and Motion," *Journal of Meteorology*, vol. 16, No. 2, Apr. 1959, pp. 121-139.
- R. G. Beebe, "Notes on the Scottsbluff, Nebraska Tornadoes, 27 June 1955," *Bulletin of the American Meteorological Society*, vol. 40, No. 3, Mar. 1959, pp. 109-116.
- R. D. Blood [with R. J. Hildreth], "Late Spring and Early Fall Low Temperatures in Texas," *Miscellaneous Publication* 298, Texas Agricultural Experiment Station, Texas Agricultural Extension Service, College Station, Texas, 1958.
- G. N. Brancato, "St. Louis Tornado, 10 February 1959," *Weatherwise*, vol. 12, No. 2, Apr. 1959, pp. 43-44.
- R. B. Carson, "Observations on the Utility, the Limitations, and the Didactic Value of Synoptic Streamline Analysis," *Transactions of the New York Academy of Sciences*, Ser. II, vol. 20, No. 7, May 1958, pp. 657-677.
- C. V. Cunniff, "Solar Radiation on the Walls Facing North and South at the Blue Hill Observatory," *Air Conditioning, Heating, and Ventilating*, vol. 56, No. 8, Aug. 1959, pp. 64-67.
- H. L. Elser, "A Desert Dust Storm Strikes El Paso, Texas," *Weatherwise*, vol. 12, No. 3, June 1959, pp. 115-116.
- I. Enger, "Singularities in Daily Temperatures," *Journal of Meteorology*, vol. 16, No. 3, June 1959, pp. 238-243.
- E. Flowers, "Inside Antarctica—No. 2, Amundsen-Scott Station," *Weatherwise*, vol. 11, No. 5, Oct. 1958, pp. 166-171, 180.
- S. Fritz, "Transmission of Solar Energy Through the Earth's Clear and Cloudy Atmosphere," *Transactions of the Conference on the Use of Solar Energy—The Scientific Basis*, Tucson, Ariz., Oct. 31-Nov. 1, 1955, The University of Arizona Press, 1958, pp. 17-36.
- B. W. Harlen, "Inside Antarctica—No. 1, Little America," *Weatherwise*, vol. 11, No. 4, Aug. 1958, pp. 116-123.
- M. F. Harris, "An Evaluation of 12-hour Statistical Forecasts of the 1000 to 500 Mb. Thickness," *Journal of Meteorology*, vol. 16, No. 1, Feb. 1959, pp. 1-5.
- L. Holloway, "Smoothing and Filtering of Time Series and Space Fields," *Advances in Geophysics*, vol. 4, Academic Press, New York, 1958, pp. 351-388.
- L. F. Hubert, "Distribution of Surface Friction in Hurricanes," *Journal of Meteorology*, vol. 16, No. 4, Aug. 1959, pp. 393-404.
- D. L. Jorgensen, "Prediction of Hurricane Motion with Use of Orthogonal Polynomials," *Journal of Meteorology*, vol. 16, No. 1, Feb. 1959, pp. 21-29.
- D. W. Krueger, "A Relation Between the Mass Circulation Through Hurricanes and Their Intensity," *Bulletin of the American Meteorological Society*, vol. 40, No. 4, Apr. 1959, pp. 182-189.
- H. E. Landsberg, Review of "Physikalisch-Statistische Regeln als Grundlagen für Wetter- und Witterungsvorhersagen," *Bulletin of the American Meteorological Society*, vol. 40, No. 4, Apr. 1959, pp. 213-214.
- J. T. Lee, "Forecasting Tornado Possibilities," *Weatherwise*, vol. 11, No. 2, Apr. 1958, p. 51.
- L. Machta [with F. Hagemann, J. Gray, Jr., and A. Turkevich], "The Stratospheric Content of Carbon-14, Carbon Dioxide and Tritium," *Science*, vol. 130, No. 3375, 4 Sept. 1959, pp. 542-552.
- W. B. Moreland, "Inside Antarctica—No. 3, The Weather Central at Little America," *Weatherwise*, vol. 11, No. 6, Dec. 1958, pp. 196-200.
- J. Namias, "Recent Seasonal Interactions Between North Pacific Waters and the Overlying Atmospheric Circulation," *Journal of Geophysical Research*, vol. 64, No. 6, June 1959, pp. 631-646.
- J. F. O'Connor, "1958—The Warmest Year on Record on the Pacific Coast," *Weatherwise*, vol. 12, No. 2, Apr. 1959, pp. 52-55, 61.
- E. Sable, "Insured Rainfall Frequency," *The Standard*, Boston, vol. 163, No. 11, Sept. 1958, p. 5.
- W. Smith, "Mesoanalysis of the Tornado-Producing Situation in Texas, 25-26 May 1955," *Bulletin of the American Meteorological Society*, vol. 40, No. 3, Mar. 1959, pp. 134-145.
- K. Tillotson, "Description of Fraser, Colorado," *Weatherwise*, vol. 11, No. 6, Dec. 1958, pp. 209-210.
- G. F. Von Eschen, "Climatic Trends in New Mexico," *Weatherwise*, vol. 11, No. 6, Dec. 1958, pp. 191-195.
- H. Wexler, "Modifying Weather on a Large Scale," *Science*, vol. 3331, Oct. 31, 1958, pp. 1059-1063.
- R. A. Wrightson, "The Blizzard of '88," *Weatherwise*, vol. 11, No. 6, Dec. 1958, pp. 187-190.